CLM-R224

CLM-R224

UKAEA

Report

CULHAM LABORATORY LIBRARY
25 JUN 1982

THE TOROIDAL FIELD COIL STRUCTURE FOR THE CULHAM MARK II C TOKAMAK REACTOR

CULHAM LIBRARY
REFERENCE ONLY

S. F. CALVERT
D. H. PROTHERO
W. R. SPEARS

CULHAM LABORATORY
Abingdon Oxfordshire
1982

C.18 Available from H. M. Stationery Office £3.00

© - UNITED KINGDOM ATOMIC ENERGY AUTHORITY - 1982
Enquiries about copyright and reproduction should be addressed to the Librarian, UKAEA, Culham Laboratory, Abingdon, Oxon. OX14 3DB, England.

THE TOROIDAL FIELD COIL STRUCTURE FOR THE CULHAM MARK II C TOKAMAK REACTOR

S.F. Calvert and D.H. Prothero
International Research & Development Co Ltd
Fossway, Newcastle upon Tyne

W.R. Spears
Culham Laboratory, Abingdon, Oxon, OX14 3DB, UK
(Euratom/UKAEA Fusion Association)

ABSTRACT

This report describes a design study carried out on the toroidal field coil system of the Culham Mark II C Conceptual Tokamak Reactor. A preliminary design is described which enabled a support structure for the toroidal field coils to be evolved. A description is given of the finite element computer model used to analyse the stresses and deflections in the coils and support structure. The results obtained from this model are discussed in detail. The importance of the constraints placed on the design of the structure by maintenance and access requirements is also assessed.

ISBN: 0 85311 107 3

CONTENTS

		Page No.
1	INTRODUCTION	1
2	INPUT DATA	1
	2.1 Coil and conductor data	1
	2.2 Loading cases	2
	2.3 Material data	3
3	PRELIMINARY ANALYSIS	4
	3.1 Analytical tools	4
	3.2 Results of analysis	4
	3.3 Proposed support structure	5
4	DETAILED STRUCTURAL ANALYSIS	6
5	RESULTS AND DISCUSSION	8
	5.1 Deflections	8
	5.2 Stresses	10
	5.2.1 Coil stresses	10
	5.2.2 Support structure stresses	11
	5.2.3 Other stresses	11
	5.3 Implication of cyclic loading	13
6	ASPECTS OF DETAILED DESIGN	14
	6.1 Insulated dowels	14
	6.2 Implications of toroidal field coil failure (loading case L4)	15
	6.3 Stresses due to mass support	17
7	TOWARDS AN IMPROVED STRUCTURE	18
8	CONCLUSIONS	20
	8.1 Deflections	20
	8.2 Stresses	21
	8.3 General design	21
9	ACKNOWLEDGEMENTS	22
	REFERENCES	22

1 INTRODUCTION

This report describes the results of a study carried out by International Research and Development Company Limited (IRD), with Culham Laboratory, into the toroidal field coil support structure of the Culham Conceptual Tokamak Reactor Mark II C. This Tokamak[1] was developed from two previous Culham Tokamak studies, the Mark II A and Mark II B Tokamaks. These studies assumed quasi steady-state operation and the latter included a single null poloidal diverter. For the present Mark II C design, pulsed operation has been assumed and the parameters relating to the pulsing of the Tokamak have been considered in greater detail; otherwise the same engineering features and roughly the same plasma parameters (i.e. cross-section, aspect ratio and plasma pressure ratio) have been used as for the previous studies. *Table 1* summarises the reactor parameters for the Culham Mark II C Tokamak and *Table 2* gives details of the toroidal field windings, which were the subject of the present study.

During its operational life a toroidal field coil will be subjected to various loadings. Some of these arise due to normal operation of the Tokamak, and others are due to faults. The various loading cases considered during the present study are explained in detail in *Section 2*.

The principal aim of the present study was to design a support structure for the toroidal field coils consistent with the requirements of reactor assembly and maintenance. At regular intervals it will be necessary to remove segments of the blanket which have become heavily irradiated. To enable this to take place, sufficient room must be left between the outer limbs of the toroidal field coils for radial removal of the blanket segments. This restricts the region in which coil support structure can be provided. Support location is further restricted by the need to provide access to structures inside the toroidal field coils for coolant ducts, other supports and instrumentation connections (see *Section 2*).

The input data used during the course of the study is described in *Section 2*. A preliminary analysis, described in *Section 3*, was first carried out to assess the stresses and deflections experienced by the coil during the various loading cases. This was used to devise a support structure for the coil system which was analysed using a finite element model. A description is given of the model used (see *Section 4*) and the results obtained from it (see *Sections 5* and *6*). The results are also used to indicate ways in which the proposed structure could be improved (see *Section 7*).

2 INPUT DATA

2.1 Coil and conductor data

The Culham Mark II C Tokamak Reactor[1] is a conceptual design in which the plasma burn time is 27 s and the time between plasma burns is 14 s. During its lifetime the Tokamak is subjected to 2×10^7 such cycles, during which the toroidal field coils are operated in a

steady state mode. The Tokamak incorporates 20 D-shaped toroidal field coils. The upper half of one coil is shown in elevation in *Figure 2.1*. A region of 150 mm is available around each coil for cryostat plus support structure along the complete length of the coil. However, no further structure can be added in the region shown shaded in *Figure 2.1*, and at the top and bottom of the coil approximately 50% of the space between coils must be free of structure. This is a result of the maintenance and access restrictions mentioned above.

For the present report the co-ordinate system shown in *Figure 2.1* is used throughout.

The conductor[2] for the toroidal field coils is a strip configuration, wound like a watch spring in the plane of the coil. *Figure 2.2* is a sketch of a typical conductor, taken from *Reference 2*. In the present study, somewhat different dimensions were chosen for the conductor. The width of the conductor in the Z direction is 0.425 m, i.e. the same as that of the coil. *Table 3* gives data relating to the toroidal field coil conductor.

2.2 Loading cases

The forces usually acting on a toroidal field coil arise in three ways:

(a) a radial outward force, due to the coil's own field, resulting in a tendency for the coil to grow,

(b) a tilting moment, due to the interaction of the coil current with the poloidal field and plasma, tending to cause the coil to adopt a horizontal attitude,

(c) a net inward force towards the machine centre-line due to interaction with neighbouring toroidal field coils.

Forces (a) and (c) act in the plane of the coil whereas the force producing (b) acts perpendicular to the coil plane. For this study the following loading conditions were considered.

L1 Normal operation during the plasma burn
- the forces act as described above.

L2 Normal operation between plasma burns
- forces (a) and (c) are present, and (b) is negligible.

L3 Sudden disappearance of plasma current
- this is similar to L1 but with increased tilting moment.

L4 One adjacent toroidal field coil carrying less than 100% of its usual current during the plasma burn
- this is similar to L1 but with an additional net out-of-plane force acting over the face of the adjacent toroidal field coil.

L5 One adjacent toroidal field coil carrying less than 100% of its usual current between plasma burns
- this is similar to L2 but with an additional net out-of-plane force acting over the face of the adjacent toroidal field coil.

During normal operation the loading conditions alternate between L1 and L2. L3 is expected to be relatively rare but the support structure has been developed to survive this loading condition. The extent to which this structure can withstand loading cases L4 and L5, is examined in *Section 6.2*.

In each of the situations described above values of the body force acting at 1525 points throughout the upper half of the toroidal field coil were obtained. These points were grouped on 61 nodal planes numbered 1 to 31 in steps of 0.5 along the coil length (see *Figure 2.1*), with 25 points over the cross-section of the coil. The calculation was performed using the programme TOK at the Rutherford Laboratory[3]. From these body forces the force per unit coil length was obtained, and values for loading cases L1 and L3 are shown in *Table 4*. Values for case L2 are identical to those for L1 but with negligible out-of-plane force (FZ).

2.3 Material data

As noted in *Table 3*, the main reinforcement envisaged within the coil winding is provided by copper-zirconium, a precipitation hardened form of copper. Material data[4] are available for one form of copper-zirconium - the proprietary alloy 'Amzirc' marketed by Amax Inc. The data relevant to this study are summarised in *Table 5*.

Based on present day practice, stainless steel is the preferred material for the support structure, as considerable experience exists in its use in large structures and there is a large amount of data on its mechanical properties at low temperature. However, no substantial continuous toroidal electrical path is permitted around the support structure. Hence, electrically insulating spacers are required with a steel structure which are unnecessary for non-metallic alternatives such as concrete or carbon fibre. In spite of this disadvantage, it was decided to proceed with the design of a structure fabricated from stainless steel, as the behaviour of this material under the given loading conditions is much better known than that of its rivals. Consideration has concentrated solely on the use of AISI 316 LN stainless steel. This material has been selected for the following reasons:

(a) it has a high strength (see *Figure 2.3*) at liquid helium temperatures,

(b) it, and related steels, have been widely used at cryogenic temperatures.

A significant amount of data exist for AISI 316 LN and for related steels. *Figure 2.4* shows a stress-strain curve measured, at 4.2 K, by the Rutherford Laboratory, on a sample of AISI 316 LN from a

forging provided by IRD. The stress-strain curve is linear for stresses up to 600 N/mm^2 and strains of 0.3%. The 0.2% proof stress (i.e. the stress which results in a permanent off-set of 0.2%) is about 1000 N/mm^2 for the annealed material. *Figure 2.3* shows the effect that cold work has on increasing the strength of AISI 316 LN.

3 PRELIMINARY ANALYSIS

A preliminary analysis, described in this section, using a simple computer program supported by hand calculations, was first carried out in order to evolve a structure for supporting the toroidal field coils. This structure was then analysed using a detailed finite element model as described in subsequent sections of this report.

3.1 Analytical tools

The main tool used in this preliminary analysis was the computer program SAGS. This is a finite element code written by the Structural Dynamics Research Corporation (SDRC). The stress analysis was carried out by sub-dividing the coil into 120 beam elements, with lumped property values (cross-sectional area, second moment of area, tensile modulus) assigned to the beams. The joints between the beams corresponded to the nodal planes in the calculation of the coil forces (see *Section 2*).

Advantage was taken of the geometrical symmetry about the horizontal mid-plane to restrict the modelling to one half of the coil (between nodal planes 1.0 and 31.0). It was assumed that the coil is restrained in the Z direction between nodes 1.0 and 25.0, where support structure between the coils is allowed. No restraint in the Z direction was imposed between nodal planes 25.0 and 31.0, where no inter-coil structure is allowed. No external restraint was imposed on growth of the coil in its own plane. This last assumption was found in the subsequent detailed finite element analysis to give somewhat misleading results (see discussion in *Section 5.2.1*).

The presence of a steel jacket surrounding the unsupported part of the coil was modelled by modifying (see *Appendix A*) the lumped property values (particularly the second moment of area). In calculating the revised values, the coil was treated as though it were bonded to the steel jacket.

3.2 Results of analysis

From the results given by SAGS, it was possible to deduce the following stresses in the coil:

(a) the direct (hoop) stress,

(b) the in-plane bending stress. (For a properly designed D-shaped coil this should be small.)

(c) the out-of-plane bending stress due to the coil forces acting in the Z direction.

These stresses can be combined simply by addition.

Similarly, those stresses, (a), (b) and (c) in the steel jacket between nodal planes 25.0 and 31.0 can also be estimated.

Figure 3.1 shows the variation of the stresses along the coil for loading case L1 assuming a steel jacket thickness of 100 mm. The hoop stress is reasonably constant at about 110 N/mm^2 and the in-plane bending moment small, confirming that the D-shaped toroidal field coils have been correctly designed. The out-of-plane bending moment is significant between nodal planes 25.0 and 31.0 where the coil is unrestrained.

Figure 3.2 shows how the peak stress in the coil and steel varies with the thickness of the steel jacket for loading case L1. It was decided that a thickness of 100 mm would be necessary to maintain the stresses in the coil at a reasonable level. Hence this thickness was chosen for the more detailed finite element analysis. This leaves 50 mm to accommodate the vacuum vessel surrounding the coil. Although the vacuum vessel was not considered in detail during the present study, this thickness allowance was considered to be adequate.

Calculations showed that for all loading cases considered, a magnetic force of approximately 360 MN acts on each coil tending to move it towards the machine centre-line. This must be resisted by a cylindrical structure which must not be electrically continuous otherwise a circulating current would be set up which would screen the plasma from the poloidal field. Consideration was given first to fabricating the central support structure from an electrically insulating material such as concrete or carbon fibre composite; however, it was decided that this route would require a large development effort with no great probability at present of ultimate success. Hence the preferred solution was to fabricate the support structure from AISI 316 LN stainless steel with the required insulation being provided by an insulating medium at the vertical planes between adjacent segments of the structure. This is essentially the solution adopted for JET[5], although the stresses involved in the present application are significantly larger. It was decided that the maximum tolerable hoop compressive stress in the central support cylinder (due to the 360 MN inward force on each coil) was 50 N/mm^2. This value is governed by the likely compressive strength of the insulation. To achieve this figure, a radial thickness of 1500 mm was required for the central support cylinder.

3.3 Proposed support structure

The support structure which evolved out of these considerations is shown in *Figures 3.3* and *3.4*. The region of the coils between nodal planes 25.0 and 31.0 is surrounded by a stainless steel box as previously described. A central support cylinder is formed by tapering the steel box around the straight section of the toroidal field coils, producing a keystone arch structure from the abutting coils, (see *Figure 3.5*).

The tilting moment in the out-of-plane direction is more difficult to react since it has the same sense for all coils and hence the coils cannot easily be reacted against one another. The method chosen was to transmit the out-of-plane forces into the central support cylinder as a torsional load by means of a substantial structure between the toroidal field coils.

The final form of the support structure largely follows the profile of the toroidal field coils although there is a variation from this shape at the top and bottom of the coils where the close proximity of poloidal field coils dictates a flattening of the structure. The poloidal field coils also define the inside diameter of the central support cylinder since it is desirable both for assembly and repair to obtain access to these coils without disturbing the toroidal field coils. To ensure that the full 11 m vertical clearance is available between adjacent toroidal field coils the inner edge of the support structure has been foreshortened by means of a chamfer (see *Figure 3.3*). At the top and bottom of the structure a space exists in order to allow access to internal structures (see *Figure 3.6*).

The need for toroidal insulation has been considered during the design. To this end the structure around each toroidal field coil forms a segment of the whole structure and is electrically insulated from its neighbours by a suitably reinforced insulating medium. Since the structure is required to be torsionally stiff to resist the out-of-plane forces on the coils the shear forces on the insulated joints must be resisted by locking the individual segments together. This could be achieved by the use of insulated dowels, or providing a surface profile on the segment faces which would result in an interlocking structure, (see *Figure 3.7*).

The proposed structure as modelled consists of a homogeneous steel support structure enclosing the toroidal field coil. In practice it would not be possible to provide a steel structure of the thickness required in one piece. Consequently, an actual design for construction would, in places, be fabricated from many layers of steel plate with the use of castings and forgings where appropriate. At this stage of the design it was not considered appropriate to take account of these constructional details. Also evident in the drawings of the support structure are a number of sharp corners. These are due to the finite element modelling requirements and are explained in *Section 4*.

4 DETAILED STRUCTURAL ANALYSIS

The complexity of the toroidal field coil support structure described in *Section 3*, and the loading conditions to be examined, required a more rigorous method of analysis than would be possible by hand calculation. Consequently, a finite element analysis method was chosen to examine the behaviour of the toroidal field coil and its associated support structure. An SDRC computer programme, SUPERB, was therefore chosen for the detailed structural analysis.

This program includes an extensive library of isoparametric, three dimensional, elements which enable large and complex structures to

be modelled using relatively few elements since the sides of the elements may be curved. The toroidal field coil and its surrounding support structure were modelled using solid, parabolic elements with three nodes on each side. While the material properties of the steel support structure were entered as a conventional, isotropic structure, advantage was taken of a feature of SUPERB which enabled the coil to be modelled as an orthotropic material. The material properties used are given in *Table 6* and derived in *Appendix A*. The size, and consequently the cost, of the SUPERB model was limited by making a number of simplifying assumptions and taking full advantage of symmetry. By ignoring the presence of the mass support, which preliminary calculations showed had only a small effect on coil and structure stress values (see *Appendix B*) it was possible to reduce the size of the model to cover the top half of a toroidal field coil only. The model was further simplified to cover a segment of the structure from the vertical mid-plane of the toroidal field coil to a plane mid-way between adjacent toroidal field coils, in fact the insulated joint referred to in *Section 3*. A major assumption that was made to reduce the complexity of the finite element model was to consider the coil/support structure interface capable of transmitting all shear, compressive and tensile loads without relative movement between the two components. Whilst it may be possible to envisage a bond capable of withstanding the shear and compressive loads the possibility of transmitting tensile loads from the coil into the support structure is clearly less feasible. However, it was felt that the reduced complexity of the model at this stage justified such an assumption. To reduce the total number of elements in the model a number of sharp corners and abrupt changes in section have been modelled where in practice smooth transitions would be provided. Because of this a careful assessment of the results of the analysis was required to discount the high stresses at these unrealistic boundaries.

The development of the finite element model is shown in *Figures 4.1, 4.2* and *4.3*. *Figure 4.1* shows the elements representing one half of the toroidal field coil. *Figure 4.2* shows the toroidal field coil surrounded by the steel support structure which is complete up to the inner radius of the access duct. *Figure 4.3* shows the complete SUPERB model of one half of the toroidal field coil and its support structure.

To evaluate the stresses and deflections using the above model symmetric loadings must be dealt with separately from antisymmetric loadings. The results of the separate analyses can then be combined in the appropriate way to provide the complete solution throughout the coil under the various loading conditions. The boundary conditions are different for each type of loading. For symmetric loads produced by in plane forces, the XY planes (see *Figure 2.1*) of the model are constrained in the Z direction and the YZ symmetry plane is restrained in the X direction. For antisymmetric loads resulting from out-of-plane forces the XY planes are restrained in both X and Y directions whereas the YZ symmetry plane is restrained in both Y and Z directions.

The results of the finite element analysis provided magnitudes of deflections and stresses in the three co-ordinate axes, shear

stresses, principal stress values and Von Mises[6] combined stress. The principal stress values were particularly useful in examining the toroidal field coil since they coincided with the axes of the coil i.e. along the coil (1), radially across the coil insulation (2) and out-of-plane across the coil (3). The Von Mises combined stress, σ is related to the three principal stresses, σ_1, σ_2, and σ_3 as follows:

$$\sigma = \sqrt{\frac{(\sigma_1 - \sigma_2)^2 + (\sigma_2 - \sigma_3)^2 + (\sigma_3 - \sigma_1)^2}{2}} \qquad (1)$$

Under steady loads σ should everywhere be less than the yield stress to ensure that failure does not occur. Hence the calculation of σ enables the factor of safety in a design to be assessed. This was useful for examining the behaviour of the steel structure. It was not used to assess the stresses in the coil, since the highly anisotropic nature of the coil made use of the Von Mises criterion highly suspect.

RESULTS AND DISCUSSION

The results obtained from the computer calculations have been analysed to give data on a number of aspects of the design. The present section considers the basic output data (deflections and stresses) obtained from the program. The following section considers that output which relates to detailed aspects of the design (e.g. mass support system, fault conditions, etc.).

5.1 Deflections

The identical in-plane deflection along the coil and structure for the loading cases L1, L2 and L3 are represented in *Figure 5.1*. *Figure 5.2* profiles the out-of-plane deflections along the coil for loading cases L1 and L3. The out-of-plane deflections are virtually zero for case L2 as the out-of-plane forces are considerably reduced.

These deflection profiles show the change in position of all parts of the toroidal field coils and structure when energised by treating as fixed the intersection of the centre-line of the machine with the horizontal coil mid-plane.

The magnitude of the in-plane deflections are small (3 mm or less) in regions where the coil is supported by a massive support structure. Where the coil is unsupported (i.e. between nodal planes 25.0 and 31.0) the deflections increase (to nearly 8 mm) due to bending. This difference is due to the large variation in hoop stress (see *Section 5.2*) which occurs because of the steel thickness limitations in each region. Thickening the steel inside and outside the coil in the unsupported region reduces this difference and to some extent this could be accommodated within the present access constraints.

The out-of-plane deflections for loading cases L1 and L3 are much larger than the in-plane deflections. These deflections can be analysed into the following three components:

(a) that due to the out-of-plane moment generated by the tilting forces causing torsion in the central support cylinder, and producing rotation of the support structure at the top and bottom of the coils,

(b) that due to bending of the support structures at the top and bottom of the coils due to the out-of-plane forces,

(c) that due to bending of the unsupported part of the coil due to the out-of-plane forces.

Hand calculations which are summarised in *Appendix C*, give a similar pattern of deflections to those shown in *Figure 5.2* and indicate that (a) provides the dominant contribution to the coil deflections. Of the remaining two contributions, the deflection due to (b) is smaller than that due to (c).

Hence, if it is desired to reduce the out-of-plane deflection of the system under loading cases L1 and L3, it is necessary to reduce the torsion in the central support cylinder (Θ in equation (C.1) of *Appendix C*). In practice, the most direct way of achieving this would be to increase the outer radius b of the central support cylinder. *Figure 5.3* shows the variation with b of the maximum out-of-plane deflection, assuming that a, Γ, ℓ, G, have the values given in *Appendix C*. The deflection would be approximately halved if the effective outer radius of the cylinder were increased from 4.15 to 4.9 m. However, with b = 4.15 m, the keystone arch already penetrates into the vacuum envelope; hence a further increase in b would require a re-design of the plasma vacuum envelope.

The out-of-plane deflections could also be reduced by means of a mechanically continuous cylinder attached to the outer part of the toroidal field coils and to the steel structure at the top and bottom of the coils. This would significantly increase the torsional stiffness of the system (effectively by increasing (b^4 - a^4) in equation (C.1). However, this method contravenes the access requirements, since such a stiff cylinder could not be readily demountable. Hence, this option has not been considered in the present study.

Figure 5.2 shows that less than 5 mm out of the total 35 mm coil deflection for case L3 is due to bending of the unsupported part of the coil. Hence, only limited benefits would be obtained by thickening the steel jacket around the coil in this region (which would contravene the access requirements), or introducing demountable struts between the outer parts of the toroidal field coils.

The size of the out-of-plane deflections described above produce additional access constraints. For example the coolant duct (located approximately 13-15 m along the coil circumference) must be capable of tolerating a deflection in the surrounding structure of 25 mm.

5.2 Stresses

The deflections described in *Section 5.1* generate stresses in the load bearing members of the toroidal field system (i.e. the copper-zirconium of the conductor, and the AISI 316 LN stainless steel support structure). In addition to these stresses some compressive stresses also occur in the inter-turn insulation in the toroidal field coils and in the insulation around the stainless steel dowels. In neither case is it possible to specify a recommended material at present. However, values of the compressive stresses around the dowels are given in *Section 6.1* of this report.

5.2.1 Coil stresses

The in-plane forces generate a hoop stress in the coil. The D-shape of the toroidal field coil has been chosen so that in the absence of any support structure, a uniform hoop tension would exist within the coil (see also *Section 3.2*). However, for the present study, a substantial structure has been introduced to support the top and bottom of the coils, but in order to allow access to the blanket segment no substantial structure exists at the outside of the coils. One consequence of this is that the hoop stress is no longer uniform throughout the coil. *Figure 5.4* plots the mean coil hoop stress over the coil perimeter, for loading case L1, as determined by the finite element program SUPERB. The variation of hoop stress for loading cases L2 and L3 is identical to that shown in *Figure 5.4*.

In the absence of any support structure a constant mean hoop tension of 110 N/mm^2, as predicted by SAGS (see *Section 3.2*) should exist along the coil. *Figure 5.4* shows that the actual stress closely approaches this value in the region where the coil is unsupported. Where the coil is supported, however, the hoop stress falls considerably - to about 20 N/mm^2 at the top and bottom of the coils and about 40 N/mm^2 at the inner limb of the coil, where it presses against the central support cylinder. Hence, a variation in the size of the support structure around the coil means that the coil hoop stress is no longer constant along its perimeter.

In the region where the coil is unsupported, bending stresses occur due to both in-plane and out-of-plane forces. The effect of the in-plane bending stresses is particularly evident in the stress distribution at nodal plane 31.0 shown in *Table 7*. The effect of the magnetic forces is to generate hoop stresses which are greater at the inside of the coil than at the outside. However, *Table 7* shows that the in-plane bending due to the in-plane forces has reversed this pattern.

The stresses in the copper-zirconium are everywhere expected to be less than 300 N/mm^2 (even when allowance is made for thermal and coil mass support stresses detailed in *Section 5.2.3*). From the data given in *Table 5*, these stresses are within the capability of commercially available copper-zirconium. These stresses imply strains of about 0.25% or less. Experimental data on niobium-tin[7] indicate that this material can withstand strains of this magnitude without a serious loss in current carrying capacity. Hence, the use of niobium-tin under these conditions appears to present no problems.

5.2.2 Support structure stresses

The support structure proposed has been analysed taking into account the material properties of AISI 316 LN stainless steel summarised in *Section 2* of the present report. This material has a high yield stress at 4 K, the temperature of the coil and support structure during operation of the Tokamak, and at this temperature the 0.2% proof stress attains a value of 1000 N/mm^2 (see *Figure 2.3*).

Between nodal planes 25.0 and 31.0 the in-plane variation of hoop stress in the support structure follows that of the coil but the magnitude is increased by the ratio of the steel and copper elastic moduli due to the perfect bond assumed between these components. The unsupported region of the toroidal field coil also experiences large bending stresses due to the out-of-plane forces present in loading cases L1 and L3. The highest stress levels in the entire steel structure are found in the support jacket between nodal planes 25.0 and 31.0. *Table 8* gives the hoop stresses, for loading cases L1, L2 and L3 occurring at the inboard edge of nodal plane 28.0 (i.e. midway between the centre of the unsupported region and the end of the massive support structure. The high tensile stress of 345 N/mm^2 for loading case L1 is over a third of the 0.2% proof stress at 4 K. Under the conditions of loading case L2 the out-of-plane force reduces to zero removing the bending stress and leaving a near constant hoop stress of approximately 170 N/mm^2 across the section.

Table 9 shows the hoop stress distribution in the out-of-plane direction for nodal plane 18.0 which occurs at the inner radius of the upper and lower access ports. Although it has been shown that the resulting spoke structure is extremely stiff compared to the central support structure (see *Section 5.1.1*), bending stresses are evident at this point for loading condition L1 and L3. This bending gives rise to an increase of hoop stress at the edge of the access port of 90 N/mm^2 over that obtained for loading case L2. A simple hand calculation treating the spoke as an encastré (no rotation) beam with a guided free end confirms this stress value.

To illustrate the stress variation along the steel structure, *Table 10* gives values of the principal stresses (σ_1, σ_2 and σ_3) and Von Mises stress at the point at each of the various nodal planes in the system where the largest Von Mises stress occurs for loading case L1. The same point at each nodal plane is chosen for all cases. These data again demonstrate that the maximum stress levels are obtained over the unsupported part of the coil with much reduced values throughout the rest of the support structure.

5.2.3 Other stresses

The stresses described in *Sections 5.2.1* and *5.2.2* refer to the electromagnetically induced stresses. These are the only stresses which have been modelled using the SUPERB computer program. Other stresses occur however, which can be estimated reasonably accurately by elementary means. This is done in the present section.

(i) Thermally induced stresses

Tensile stresses will be generated due to differential thermal contraction between the copper-zirconium based coil and the stainless steel support structure. At a particular point along the coil let A_c be the cross-sectional area of copper-zirconium, E_c its elastic modulus and ε_c its integrated thermal strain from room temperature (taken here as 300 K) to 4.2 K. If A_s, E_s, ε_s are the corresponding values for the steel then the thermally induced stresses, σ_c and σ_s, in copper-zirconium and steel are given by:

$$\sigma_c = \frac{E_c (\varepsilon_c - \varepsilon_s)}{\left[1 + \frac{A_c E_c}{A_s E_s}\right]} \qquad \sigma_s = \frac{-E_s (\varepsilon_c - \varepsilon_s)}{\left[1 + \frac{A_s E_s}{A_c E_c}\right]} \qquad (2)$$

Measurements carried out by Rutherford High Energy Laboratory for IRD give a value of $\varepsilon_s = 3.04 \times 10^{-3}$ for AISI 316 LN steel. Data for copper-zirconium do not appear to be available; hence a value for ε_c of 3.39×10^{-3} appropriate to pure copper has been taken. (The published data on Amzirc[4] indicates that the linear thermal contraction rate at room temperature is $1.69 \times 10^{-5}/^{o}C$, i.e. closely similar to that of copper). A value of 118 GN/m^2 has been taken for E_c and 200 GN/m^2 (see *Figure 2.4*) for E_s.

The thermal stresses have been considered in two regions.

(a) Top and bottom regions

Here the coil is surrounded by a massive steel structure of cross-sectional area approximately 5 m^2. The copper-zirconium area is approximately 0.33 m^2. Application of equations (2) give σ_c = +40 N/mm^2 and σ_s = -3 N/mm^2. The negative sign for σ_s indicates that the thermal stress in the steel is compressive.

(b) Unsupported region

In this case the coil is surrounded only by a 100 mm steel jacket of cross-sectional area 0.305 m^2. Hence in this region, σ_c = +25 N/mm^2 and σ_s = -28 N/mm^2.

These values may be compared with the electromagnetic hoop stress along the coil, profiled in *Figure 5.4*. This comparison shows that the thermal stresses are comparable to the magnetically induced stresses where the coil is solidly supported but are much smaller than the magnetic stresses where the coil is less strongly supported. The overall effect on the copper-zirconium is to reduce slightly the variation in magnetic hoop stress along the perimeter of the coil.

These thermal stresses are derived from a relatively small assumed difference (3.5×10^{-4}) in the thermal contractions of copper-zirconium and 316 LN steel. Direct measurements of the thermal contraction of copper-zirconium are clearly advisable, since

any error in the value assumed here for the thermal contraction could have a large effect on the thermal stresses.

(ii) Stress due to mass support

These are considered in detail in *Section 6.3* and *Appendix B*, where it is shown that the maximum stress due to the mass support is expected to be significantly less than 50 N/mm^2. This is much less than the peak magnetically induced stresses.

5.3 Implication of cyclic loading

During its projected lifetime, the Culham Mark II C Tokamak will be subjected to 2×10^7 operating cycles during which the poloidal field coils are alternatively energised and de-energised. Hence the toroidal field coils and the steel support structure will be subject to cyclic stresses. *Table 10* shows the maximum and minimum stress values of various points in the steel structure under normal operating conditions.

To assess the effect of these stresses during the lifetime of the machine, a full fracture mechanics assessment would be required. It is not the purpose of this section to provide such an assessment. However, a preliminary appraisal is given in *Appendix D*, largely to establish whether a detailed fracture mechanics assessment is required at the present stage of development of the structure design. Based on certain assumptions the number of cycles to failure for a point in the AISI 316 LN support structure is given by:

$$N = \frac{10^{11}}{(\Delta\sigma)^3 \sqrt{a}} \qquad (3)$$

where a is the minimum detectable crack size in metres, assumed here to be 0.003 m, and $\Delta\sigma$ is the cyclic stress variation in MN/m^2.

Equation (3) can obviously be used in conjunction with *Table 10* to estimate the number of cycles to failure for different parts of the structure. However, this procedure involves the following simplifications and approximations which are detailed below.

(a) Equation (3) is strictly valid only for a crack subjected to a cyclically varying unidirectional force. In reality, three force components are present which are varying by different amounts. However, the SUPERB results show that the stress component σ_1 dominates over the other components at all parts of the steel structure except the central support cylinder where radial compressive stresses are important. This suggests that for most of the structure equation (3) can be used with $\Delta\sigma$ taken as the difference between the values of σ_1 in loading cases L1 and L2.

(b) Fault conditions have been ignored. Hence the analysis assumes that loading cases L3, L4 and L5 do not occur, or at least, are very rare.

(c) A number of optimistic assumptions have been incorporated into the analysis. In particular, a low initial crack size has been assumed, and the line taken for crack growth rate does not include any safety factor. Both these points are amplified in *Appendix D*.

With these qualifications, equation (3) can be used to provide an estimate of the number of cycles to failure of certain parts of the steel structure and the results are shown in *Table 11*. The results indicate that, at the points considered, the structure would not, on this preliminary appraisal, tolerate 2×10^7 cycles without suffering unacceptable crack growth at various regions. Hence, this indicates that attention should be paid to the fracture mechanics aspects of the Culham Mark II C Tokamak, since it is possible that limitations or modifications of the design may be required. It should be emphasised again that this section is not intended to be a fracture mechanics assessment of the toroidal field coils and structure but has indicated the need for further work in this area. A part of the required work is experimental in nature, in particular the following:

(a) further data on AISI 316 LN to establish the threshold stress intensity range ΔK_o. Since the stress range, $\Delta\sigma$, is not large in many parts of the toroidal field system, it may be possible to design these parts so that no crack growth occurs,

(b) an experimental programme to obtain fracture mechanics data on copper-zirconium for which no experimental results appear to be available.

With this data available, it should then be possible to carry out a proper fracture mechanics assessment using a procedure such as that evolved by the CEGB[8], in which appropriate consideration is given to safety factors, flaw geometries and failure assessment and also a consideration of fault modes which may occur. These inevitably have been excluded from the treatment given in the present section.

6 ASPECTS OF DETAILED DESIGN

In the present section three aspects of the design, i.e. the insulated dowels, fault conditions and mass support arrangements are examined in some detail in order to establish their importance on the design philosophy.

6.1 Insulated dowels

The design of the proposed support structure requires all loads in the out-of-plane direction to be reacted by a torsionally stiff central support cylinder. To this end a cylinder of substantial wall thickness (approximately 1.5 m) has been designed by providing

a wedge section to the steel jacket surrounding the straight portion of each of the toroidal field coils and allowing these sections to abutt against each other (see *Figure 3.5*). No continuous toroidal electrical path should exist around the structure and thus adjacent toroidal field coil jackets must be electrically isolated from one another by means of an insulating medium over their contacting surfaces. It is necessary however, to transmit a predominantly vertical shear force across these joints to provide the torsional stiffness required. For loading case L1 the shear stress across the insulated surface has a mean value of 20 N/mm^2 (see *Appendix E*). Although tests conducted at IRD have shown that bonds with this order of shear resistance can be achieved between resin bonded steel plates it is proposed that a more definite means of mechanical interlocking between segments of the support structure should be provided. A similar problem to this has been encountered on the JET experiment[5] and, although the loads are higher in the Mark II C Tokamak, a similar solution is recommended. This requires the use of insulated dowels to provide an interlocking structure between segments of the support structure. As in the JET application the dowels are fitted such that half is embedded in each abutting segment thus taking the shear load across the diameter of the dowel. In the JET application a maximum shear stress of 150 N/mm^2, including stress concentration effects, is expected in most cases. Because of the increased strength of AISI 316 LN at 4 K, it was considered that this figure could be raised to 250 N/mm^2 for the Culham Mark II C Tokamak. A value of 2.5 was considered reasonable for the stress concentration factor; hence a working shear stress of 100 N/mm^2 was taken. To attain this value of shear stress it is necessary for 20% of the abutting area to consist of dowelling.

It was also assumed that the shear load on the dowel would be transmitted into the body of the structure through 25% of the surface area of the dowel. Hence the resulting compressive stress is 1.27 times the shear stress (see *Appendix F*), i.e. 127 N/mm^2 in the present case. For a given total dowelling area the magnitude of the shear and compressive stresses are not significantly affected by the dimensions of the dowels. Using 50 mm diameter dowels, 500 mm in length, a total of 200 dowels would be required. An optimum orientation angle for each dowel exists although for simplicity of manufacture it may be acceptable to fit the majority of dowels over the straight section of the coil in the radial direction, and the majority of those in the outer parts of the support structure in the vertical direction. This may result in a larger number of dowels to prevent unacceptable stress levels being attained. A more detailed analysis than the current one is recommended to evaluate fully the concept of insulated dowels.

The anticipated working compressive stress of 127 N/mm^2 implies a maximum stress of about 250 N/mm^2 (because of stress concentration effects). This is a high value and experimental work is required to show that suitable insulating materials exist which can withstand these loads under cyclic conditions.

6.2 Implications of toroidal field coil failure (loading case L4)

Loading case L4 occurs when the current in one of the toroidal field coils falls to zero. This has the following implications.

(a) The forces labelled (a), (b) and (c) in *Section 2.2* fall to zero in the failed coil. Under normal conditions, force component (c) is balanced by an equal and opposite outward force due to other toroidal coils pressing inwardly on the central support cylinder. During L4, therefore, a net outward force acts on the failed coil in the major radial direction.

(b) A net out-of-plane repulsive force acts between the failed coil and each of the two adjacent toroidal field coils.

During the course of the study it was realised that protection systems would probably prevent complete failure of a coil when the other coils are fully energised. However, the case of one coil carrying less than its full current still required attention, and this is done in this section.

If the outward radial force described in (a) were permitted to cause movement of the failed coil, the central support cylinder would collapse. A shear force of 180 MN (i.e. half the magnitude of the coil inward force given in *Section 3.2*) must be resisted on each abutting face of the coil support structure in the event of total coil failure. This can only be resisted by the insulated dowels. To resist the coil tilting force for cases L1 and L3, the dowels must be aligned radially along the central support cylinder. However, to resist the outward coil shear force for case L4 the dowels there must be aligned vertically. It is therefore proposed that half of the dowels along the cylinder are arranged in a vertical and half in a radial direction. This presents an area of about 3 m^2 to resist the shear force present under coil failure. An increase in shear stress, with due allowance for stress concentration effects, of 120 N/mm^2 would result. This would nearly double the shear stress in the dowels and is therefore not considered practical. *Table 12* shows the total shear stress in the dowels for various proportions of total coil failure. In practice the shear stresses due to torsion and coil failure would not be directly additive due to a difference in their direction. Thus, *Table 12* gives a pessimistic result. The maximum permissible shear stress is approximately half the 0.2% proof stress (i.e. 500-700 N/mm^2 for AISI 316 LN at 4 K, from the data given in *Figure 2.3*). Reference to *Table 12* shows that this implies that the current ratio between failing and non-failing coils should be not less than 60%, allowing a safety factor of 2 between design stress and maximum permissible shear stress.

The deflection of the support structure would be unaltered from the normal operating conditions since the net force on the toroidal field coil system remains the same. Local effects on the two coils adjacent to the failed coil would result in a considerable increase in bending of the unsupported part of the coil in the out-of-plane direction. Under loading cases L1 and L3, the maximum out-of-plane deflection due to coil bending is about 1.3 mm and occurs roughly at nodal plane 28.0 (see *Appendix C*). For loading case L4 the maximum deflection due to coil bending would increase to about 30 mm and would occur at nodal plane 31.0. These deflections are in addition to the deflection due to torsion in the support structure.

For a partial coil failure, where the current in an adjacent coil is reduced by a fraction f, the deflection due to coil bending would be the same fraction f of the deflection for loading case L4. For example, a 40% coil current reduction (i.e. the failed coil carrying 60% of its normal current) would cause a deflection of about 12 mm at nodal plane 31.0 on the neighbouring coils.

6.3 Stresses due to mass support

Table 13 gives a breakdown of the total mass of the coils and support structure considered for this report. The entire mass of the system is about 15000 tonnes, giving a mass of 750 tonnes associated with each of the 20 toroidal field coils in the Tokamak. The mass associated with each toroidal field coil is supported by the structure shown in *Figure 6.1*. The coil and structure rest on an epoxy pad, which in turn rests on a steel pedestal. The position shown in *Figure 6.1* was chosen for the pedestal because of the absence of poloidal field coils in this region. The pedestal would be supported on a system of rollers to allow movement both in the plane of the coil and in the toroidal direction. The displacements expected in the plane of the coil are as follows:

(a) A movement of about 30 mm towards the axis of the Tokamak due to thermal contraction of the toroidal field coil and support system during cooldown from room temperature to 4 K.

(b) A movement of about 1 mm away from the axis of the Tokamak due to growth of the toroidal field coil when loaded magnetically. This displacement is clearly negligible compared with (a).

The out-of-plane deflection which must be accommodated is also due to electromagnetic loading. At the weight support point, the out-of-plane deflection is approximately 25 mm for loading case L1 and 32 mm for loading case L3.

It is recommended that a design value of 100 N/mm^2 should be taken for the maximum compressive stress in the epoxy resin pads. Measurements at IRD on the compressive strength of epoxy impregnated coil sections indicate that epoxy resin can withstand compressive stresses up to this level. Hence, for the present application, a cross-sectional area of 0.075 m^2 is required for the epoxy resin pad. If a thickness of 30 mm is taken for the pad then the heat inleak to each coil through the epoxy will be 75 W (assuming a mean thermal conductivity of 0.1 W/mK for epoxy between 4.2 K and 300 K). This heat inleak through the supports represents 0.1 Watt per tonne of system weight. This figure could be reduced if desired by increasing the thickness of the epoxy pad. However, if it were desired to increase the thickness considerably, some attention would be required in the manufacture and stressing of the pads.

The stresses set up in the coil in the region where the Tokamak mass is supported were not considered in the computer model analysed using SUPERB since preliminary calculations indicated that the

stresses due to the mass support were small. A maximum value of 50 N/mm^2 has been calculated (see *Appendix B*).

7 TOWARDS AN IMPROVED STRUCTURE

The previous sections of this report have described a support structure system for the toroidal field coils, and the stresses and deflections in this system have been analysed in some detail. The analysis has shown areas in which the proposed structure is either doubtful or definitely inadequate. These areas are as follows.

(i) The variation in stresses during cycling is too large. Failure due to fatigue crack growth is certain for some parts of the steel structure, most particularly the steel jacket surrounding the coil in its unsupported region.

(ii) The hoop stress is not constant along the length of the coil. Hence, bending moments will occur across the winding - particularly in the region of nodal plane 25.0. This may lead to premature quenching of the coils or electrical failure of the coil inter-turn insulation.

(iii) Failure of the insulation surrounding the dowels, due to cycling, would lead to two possible faults: an electrical failure whereby the breakdown of insulation permitted screening currents to circulate around the structure, or a mechanical failure whereby movement of the dowels resulted in a breakdown of the integrity of the structure giving large deflections in the out-of-plane direction. Neither of these failures would be acceptable. At present, insufficient data exist on the fatigue life of insulating materials under the conditions expected in the Culham Mark II C Tokamak. Hence, it is not possible to establish what safety margin exists for the present design.

(iv) The net deflections of coil and support structure in the out-of-plane direction are quite large (up to 35 mm during loading case L3) but are much smaller in the plane of the coils.

An attempt has been made to list the areas (i) to (iv) in descending order of importance, although it is realised that such an assessment is subjective. The ordering is proposed on the grounds that the structure presently proposed is certain to fail due to (i) provided the assumptions in *Section 5.3* are valid, but not to any other cause. (ii) and (iii) represent possible rather than certain causes of failure. (iii) is placed below (ii) on the grounds that some scope exists within the present design for alleviating (iii) (by increasing the number of dowels and optimising their alignment), but not (ii). (iv) is placed last because the large deflections would not in themselves cause failure.

The methods by which (i) to (iv) can be alleviated within the present design constraints, are, in descending order of importance, as follows.

(a) Thickening the inside and outside of the steel jacket surrounding the coil in the unsupported region. This would alleviate problems (i) and (ii).

(b) Some scope may exist for reducing the massive structure at the top and bottom of the coils, since the stresses in these regions are low, and the fatigue conditions less onerous than in other parts of the structure. A more detailed investigation of the SUPERB results than has been possible during the present study would be necessary to establish whether this is feasible. If it is feasible however, some alleviation in problem (ii) would result.

(c) Further improvement in the alignment and disposition of the insulated dowels to reduce the stresses across the insulation to an acceptable level. (This level would have to be determined by separate tests.) This would alleviate problem (iii).

Further improvement could be made, if some initial constraints were relaxed. Again, these are set out in order of importance.

(d) A reduction in the number of cycles during the lifetime of the Tokamak from 2×10^7. This would alleviate problem (i).

(e) An increase in the space available for structure around the coil in the unsupported region would enable a thicker structure to be used and would alleviate problem (ii). With the present access requirements this would require an increase in toroidal field coil size.

(f) Thickening the central support cylinder. This would reduce out-of-plane deflections, and hence alleviate problem (iv).

(g) A complete abandonment of external access requirements would enable the out-of-plane deflections to be reduced by means of a shell on the outside of the coils. This would effectively eliminate problem (iv).

In using the model described in this report, a number of assumptions had to be made, the most important of which are given below:

(i) perfect bonding between the coil and its surrounding steel jacket,

(ii) the insulated dowels possess no elasticity,

(iii) the elastic properties of the coil have been simplified, particularly in directions transverse to the winding.

It is clearly difficult to assess the importance of these assumptions without carrying out more analytical work. However, it is believed that neither of the assumptions (i) and (iii) significantly influences the important results of this study, for the following reasons.

(a) The stiffness of the steel support structure is everywhere much greater than that of the coil against bending in both the in-plane and out-of-plane directions. Hence, if the coil were debonded from the steel, the deflections and stresses in the system would not be greatly changed. Similarly, little change in stresses and deflections would occur if debonding occurred between neighbouring turns of conductor in the coil winding. Such debonding however might lead to premature quenching of the coil if relative movement occurred between the debonded turns.

(b) The stresses in most of the system except the keystone arch support lie roughly along the direction of the conductor. The modulus of the coil in this direction is accurately known (i.e. the modulus of copper-zirconium multiplied by the fraction of copper-zirconium in the winding). The uncertainty in the effective modulus in the directions transverse to the conductor does not significantly affect the magnitude of the stresses along the conductor.

8 CONCLUSIONS

This report has described the results of a study carried out into the toroidal field coil structure of the Culham Mark II C Conceptual Tokamak design. The study has analysed the forces and calculated the stresses generated in the system using the computer package, SUPERB. The main conclusions arising out of this work are summarised below. For convenience the conclusions relating to system deflections, stresses and general design are listed separately.

8.1 Deflections

The deflection of the toroidal field coil and steel structure in the plane of the coil are similar for all the loading cases considered. (The actual deflection profile is shown in *Figure 5.1*.)

During the plasma burn the out-of-plane deflections greatly exceed the in-plane deflections. Out-of-plane deflections of up to 35 mm occur in case L3 and are only slightly smaller for case L1. These deflections are due mainly to torsion in the central support cylinder.

If it is desired to reduce the toroidal deflections in the system, one of the following two approaches should be adopted:

(i) stiffen the central support cylinder (keystone arch) by increasing its outer radius,

(ii) abandon the requirement that the coil should be unobstructed between nodal planes 25.0 and 31.0, and attach this region of each coil to a mechanically continuous cylinder around the outside of the torus.

Neither of these options can be accommodated within the present design constraints.

8.2 Stresses

In the absence of a support structure, the D-shaped toroidal field coil would experience a constant hoop tension along its perimeter due to the in-plane electromagnetic forces acting on it during operation. In the present case, however, the coil has a substantial support structure around it between nodal planes 1.0 to 25.0, and a much less substantial structure between nodal planes 25.0 and 31.0. Hence, the hoop stress in the coil is no longer uniform, but is significantly larger between nodes 25.0 to 31.0 than between nodes 1.0 to 25.0.

With the structure proposed the stresses generated are significantly below the proof stresses of the materials.

Due to the large number of cycles in the operating life of the Tokamak, and the relatively large variation in stress during cycling between loading cases L1 and L2, a serious risk exists of fatigue and subsequent crack growth in parts of the steel support structure.

No fracture mechanics assessment of the toroidal field coils has been possible due to the lack of material property data, and further investigation is recommended.

Calculations carried out on the stresses due to the coil mass support structure suggest that these are unimportant.

8.3 General design

An important feature of the design is the arrangement necessary to prevent circulating toroidal currents. The work carried out in this study suggests that the use of insulated steel dowels (as in the JET Tokamak) is a promising method of achieving this. However, further work is necessary to establish whether this method can be used to deal with the much higher forces present in the Culham Mark II C Tokamak.

The requirement that the region near the outer part of the coil, between nodal planes no. 25.0 and 31.0, should be unobstructed (to allow access for blanket segment removal) has affected the design in the following areas.

(i) It has prevented the use of an outer cylinder to restrain the out-of-plane forces (see *Section 8.1*). Hence, the toroidal deflections of the coils during loading cases L1 and L3 have been greatly increased.

(ii) The hoop stress in the coil is no longer uniform because that part of the coil between nodal planes 25.0 and 31.0 is less massively supported than the remainder of the coil (see *Section 8.2*).

If the access requirement were lifted, therefore, the overall support structure design would be modified in the following ways.

(a) A continuous cylinder on the outside of the torus and attached to all coils, would be included to reduce out of plane deflections.

(b) The steel jacket around the coil between nodal planes 25.0 and 31.0 would be increased in thickness to make the hoop stresses more uniform along the coil perimeter.

The use of demountable struts to brace neighbouring toroidal field coils along the unobstructed region would be largely ineffective in reducing the out-of-plane deflections, or making the stresses more uniform; hence their use is not considered worthwhile.

9 ACKNOWLEDGEMENTS

The authors would like to acknowledge the assistance of N.J. Diserens of Rutherford Laboratory in the calculation of the force data on which the study was based.

The authors would also like to thank Dr. R. Hancox, J.T.D. Mitchell, Dr. P. Reynolds and H. Crawley of Culham Laboratory and Dr. C.R. Walters of Rutherford Laboratory for useful discussions held during the course of the study. Thanks are also due to R. Potts of IRD for his advice during the study. The authors are deeply grateful to Dr. T. Ranshi, R. Algar, D. Parry and their colleagues at Structural Dynamics Research Corporation (SDRC) for their invaluable assistance in running the computer package, SUPERB.

REFERENCES

1 SPEARS, W.R., and HANCOX, R. A pulsed Tokamak reactor study. Culham Laboratory report CLM-R197. 1979.

2 WALTERS, C.R. Development of superconductors for fusion technology. Rutherford Laboratory report RL-77-131/A. 1977.

3 DISIRENS, N.J. TOK, users guide. Rutherford Laboratory report RL-75-111. 1975.

4 Amzirc - oxygen free copper plus zirconium. Interim publication issued by Amax Copper Inc.

5 JET project (design proposal) EUR-JET-R5. 1975.

6 PETERSON, R.E. Stress concentration factors. Wiley, 1974, p. 7.

7 DEIS, D.W., CORNISH, D.N., ROSDAKL, A.R., and HIRZEL, D.G. Mechanical strain of large filamentary Nb_3Sn conductor for fusion magnets. Proc. 6th Int. Conf. Mag. Tech., (Bratislava). 1977.

8 HARRISON, R.P., LOOSEMORE, K., and MILNE, I. Assessment of the integrity of structures containing defects. CEGB report R/H/R6. August, 1976.

TABLE 1

600 MW_e reactor reference parameters

Plasma major radius	7.8	m
Plasma minor radius	2.0	m
Plasma elongation	1.68	
Blanket/shield/ducting thickness (inner)	2.1	m
(outer)	3.8	m
Safety factor at plasma edge	2.2	
Total beta	7.7	%
Poloidal beta	2.5	
Plasma current	11.0	MA
Centre-line vacuum toroidal flux density	3.9	T
Peak fuel line density	3.1	10^{21} ions/m
Burn temperature	10	keV
Fractional burn-up	0.3	
Heating power	86	MW
Burn time	27	s
Heating time	6	s
Cycle time	41	s
Mean neutron wall loading	1.5	MW/m^2
Recoverable energy per reaction	20	MeV
Gross thermal power output	1830	MW_{th}
Thermal conversion efficiency	40	%
Recirculating power fraction	0.19	

TABLE 2

Toroidal field coil design

Total ampere turns	153	MAT
Major radius of inner limb centre-line	3.2	m
Major radius of outer limb centre-line	14.1	m
Major radius of peak height	7.0	m
Peak height of centre-line	8.4	m
Height of straight section	5.4	m
Coil radial thickness	0.9	m
Coil toroidal thickness	0.43	m
Number of coils	20	
Toroidal flux density at plasma axis	3.9	T

TABLE 3

Toroidal field coil conductor

Conductor current	29.8 kA
Number of turns	257
Thickness of conductor constituents (see also *Figure 2.2*):	
Superconductor (Nb_3Sn)	8.86 μm
Substrate (CuZr)	2.77 mm
Insulation (ceramic)	0.12 mm
Coolant (2 equal channels)	0.60 mm
Proportion of conductor constituents:	
Substrate	87.7%
Coolant	8.6%
Insulation	3.4%
Superconductor	0.3%

TABLE 4

Coil forces for loading cases L1 and L3

Nodal plane number	Force/length (meganewtons/metre)			
	Loading case L1		Loading case L3	
	FR	FZ	FR	FZ
1.0	34.29	0.0	34.29	0.0
1.5	34.29	6.54	34.29	6.94
2.0	34.29	3.99	34.29	4.73
2.5	34.29	2.40	34.29	3.39
3.0	34.29	1.84	34.29	2.96
3.5	34.29	2.04	34.29	3.19
4.0	34.60	3.02	34.60	4.10
4.5	34.76	3.47	34.76	4.32
5.0	34.71	4.04	34.70	4.67
5.5	34.57	4.51	34.53	4.94
6.0	34.27	4.83	34.27	5.07
6.5	33.92	5.20	33.92	5.26
7.0	33.50	5.60	33.50	5.49
7.5	32.97	5.56	32.97	5.30
8.0	32.40	4.76	32.40	4.36
8.5	31.79	3.74	31.79	3.21
9.0	31.15	3.35	31.15	2.69
9.5	30.47	3.87	30.47	3.12
10.0	29.74	4.84	29.74	3.99
10.5	28.89	5.63	28.89	4.70
11.0	28.06	5.97	28.06	4.97
11.5	27.24	6.07	27.24	5.00
12.0	26.44	6.05	26.44	4.93
12.5	25.65	5.96	25.65	4.79
13.0	24.85	5.74	24.85	4.53
13.5	23.90	5.18	23.90	3.95
14.0	23.03	3.73	23.03	2.48

TABLE 4 (cont'd)

Nodal plane number	Force/length (meganewtons/metre)			
	Loading case L1		Loading case L3	
	FR	FZ	FR	FZ
14.5	22.23	0.87	22.23	-0.39
15.0	21.47	-2.46	21.47	-3.73
15.5	20.74	-4.14	20.74	-5.42
16.0	20.01	-4.43	20.01	-5.72
16.5	19.16	-3.34	19.16	-4.62
17.0	18.43	-0.55	18.43	-1.81
17.5	17.76	2.16	17.76	0.92
18.0	17.15	3.27	17.15	2.04
18.5	16.57	3.28	16.57	2.06
19.0	16.00	1.96	16.00	0.76
19.5	15.34	-1.83	15.34	-3.01
20.0	14.79	-4.21	14.79	-5.36
20.5	14.31	-4.71	14.31	-5.83
21.0	13.87	-4.67	13.87	-5.76
21.5	13.46	-4.54	13.46	-5.61
22.0	13.05	-4.45	13.05	-5.49
22.5	12.60	-4.43	12.60	-5.43
23.0	12.23	-4.49	12.23	-5.45
23.5	11.92	-4.61	11.92	-5.53
24.0	11.63	-4.66	11.63	-5.54
24.5	11.37	-4.53	11.37	-5.37
25.0	11.10	-4.73	11.11	-5.53
25.5	10.84	-5.22	10.84	-5.96
26.0	10.63	-5.55	10.63	-6.24
26.5	10.45	-4.38	10.45	-5.03
27.0	10.29	-1.96	10.29	-2.53
27.5	10.15	-1.93	10.15	-2.45
28.0	10.02	-2.75	10.02	-3.20

TABLE 4 (cont'd)

Nodal plane number	Force/length (meganewtons/metre)			
	Loading case L1		Loading case L3	
	FR	FZ	FR	FZ
28.5	9.89	-3.85	9.89	-4.23
29.0	9.80	-4.93	9.80	-5.24
29.5	9.74	-5.13	9.74	-5.37
30.0	9.70	-1.48	9.70	-1.63
30.5	9.67	0.84	9.67	0.77
31.0	9.66	0.0	9.66	0.0

TABLE 5

Low temperature properties of copper-zirconium

Modulus of elasticity	118 GN/m^2
Yield strength (0.2% offset)	450 MN/m^2
Tensile strength	590 MN/m^2

TABLE 6

Assumed mechanical data for toroidal field coils

Young's modulus:	
Along coil, E_1	103 GN/m^2
Radially, E_2	59 GN/m^2
Out-of-plane direction, E_3	79 GN/m^2
Poisson's ratio:	
ν_{12}	0.26
ν_{23}	0.2
ν_{13}	0.15

TABLE 7

Hoop stress distribution
in coil nodal plane 31.0

(All stress values given in N/mm^2)

116.7	114.8	124.9	137.7	173.7
103.9		83.1		153.0
106.7	75.6	81.1	91.2	160.2
103.9		83.1		153.0
116.7	114.8	124.9	137.7	173.7

Coil mid-plane

Coil inner edge

Coil outer edge

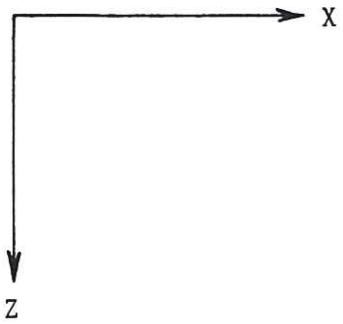

TABLE 8

Hoop stress variation across nodal plane 28.0

Node	Hoop stress L1 N/mm^2	Hoop stress L2 N/mm^2	Hoop stress L3 N/mm^2
A	13.0	168.7	13.2
B	20.9	173.0	13.4
C	84.7	173.9	70.2
D	179.4	176.8	179.5
E	274.1	173.9	288.8
F	337.9	173.0	345.6
G	345.8	168.7	345.8

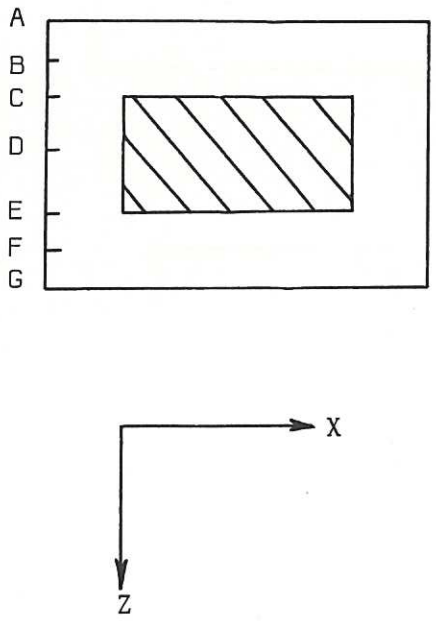

TABLE 9

Hoop stress variation across nodal plane 18.0

Node	Hoop stress L1 N/mm^2	Hoop stress L2 N/mm^2	Hoop stress L3 N/mm^2
A	147.7	54.6	163.7
B	49.0	44.3	50.1
C	-98.7	54.5	-63.6

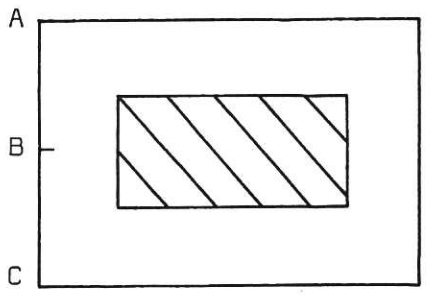

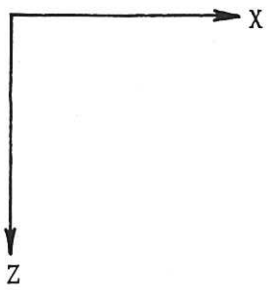

TABLE 10

Von Mises and principal stresses in steel structure

Nodal plane	Loading case L1				Loading case L2				Loading case L3			
	Von Mises N/mm^2	σ_1 N/mm^2	σ_2 N/mm^2	σ_3 N/mm^2	Von Mises N/mm^2	σ_1 N/mm^2	σ_2 N/mm^2	σ_3 N/mm^2	Von Mises N/mm^2	σ_1 N/mm^2	σ_2 N/mm^2	σ_3 N/mm^2
1.0	176.0	59.1	-140.4	-3.2	169.2	53.8	-136.6	-3.5	182.8	62.9	-143.7	-3.1
4.0	186.7	139.1	-75.0	9.7	103.7	91.1	-25.8	10.0	227.2	162.4	- 98.7	9.6
13.0	129.7	121.6	-19.8	8.2	83.8	92.4	8.0	9.3	149.4	133.6	- 31.7	8.3
18.0	133.4	172.9	38.0	41.2	38.8	42.7	3.0	4.8	149.4	195.5	43.9	48.4
22.0	68.5	70.0	-6.7	14.8	45.3	44.4	-6.0	7.1	76.2	76.6	-9.0	16.1
25.0	228.6	303.3	67.8	82.5	165.4	210.7	37.1	54.9	225.1	299.7	68.4	81.3
28.0	348.8	340.8	-26.0	14.7	180.5	175.7	-20.0	15.8	186.3	176.8	-26.6	14.5
31.0	237.0	236.9	-5.3	7.5	204.2	207.9	-0.1	7.7	206.4	206.7	-6.3	7.5

TABLE 11

Fatigue in coil support structure

Nodal plane	$\Delta\sigma$ (N/mm^2)	No. of cycles, N, to failure
13.0	29	$> 7 \times 10^7$
18.0	130	0.8×10^6
22.0	26	10×10^7
25.0	93	2.3×10^6
28.0	165	0.4×10^6
31.0	29	7×10^7

TABLE 12

Loading case L4 - dowel shear stress

Coil current (% age of normal current)	Dowel shear stress due to tilting moment (N/mm^2)	Dowel shear stress due to radial force on failed coil (N/mm^2)	Net dowel stress (excluding stress concentration factor)	Net dowel stress (including stress concentration factor)
0	100	60	160	400
20	100	48	148	370
40	100	36	136	340
60	100	24	124	310
80	100	12	112	280
90	100	6	106	265

50% of dowels aligned vertically,
50% of dowels aligned horizontally.
Assumed stress concentration allowance = 2.5.

TABLE 13

Coil and support structure mass

Element	Mass/coil tonnes	Total mass tonnes
Coil	140	2800
Central cylinder	175	3500
Spokes	108	2160
Outer ring	309	6180
Jacket on unsupported section of coil	25	500
Total mass	757	15140

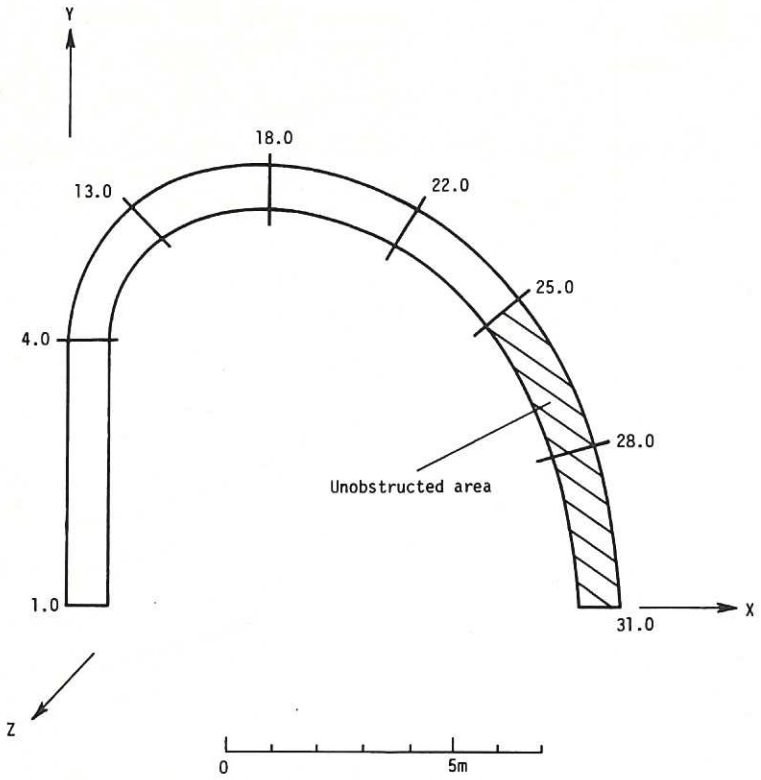

Fig.2.1 Elevation of toroidal field coil

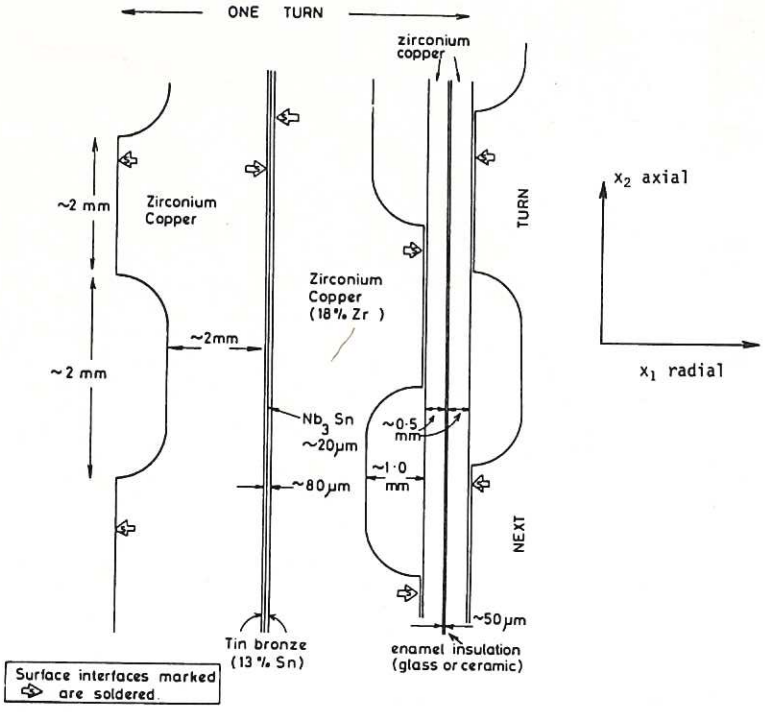

Fig.2.2 Section through proposed strip conductor

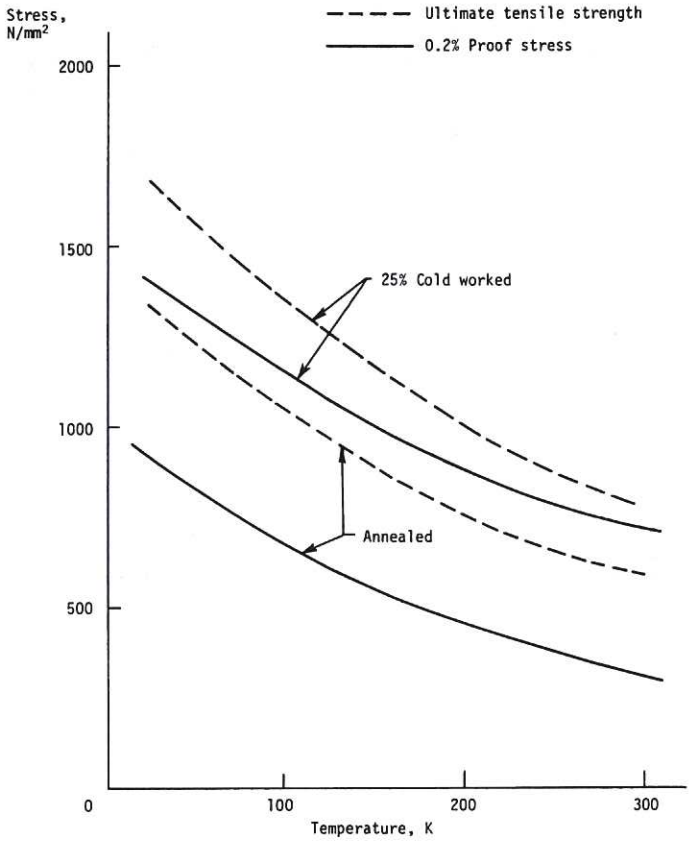

Fig.2.3 Mechanical properties of AISI 316 LN steel

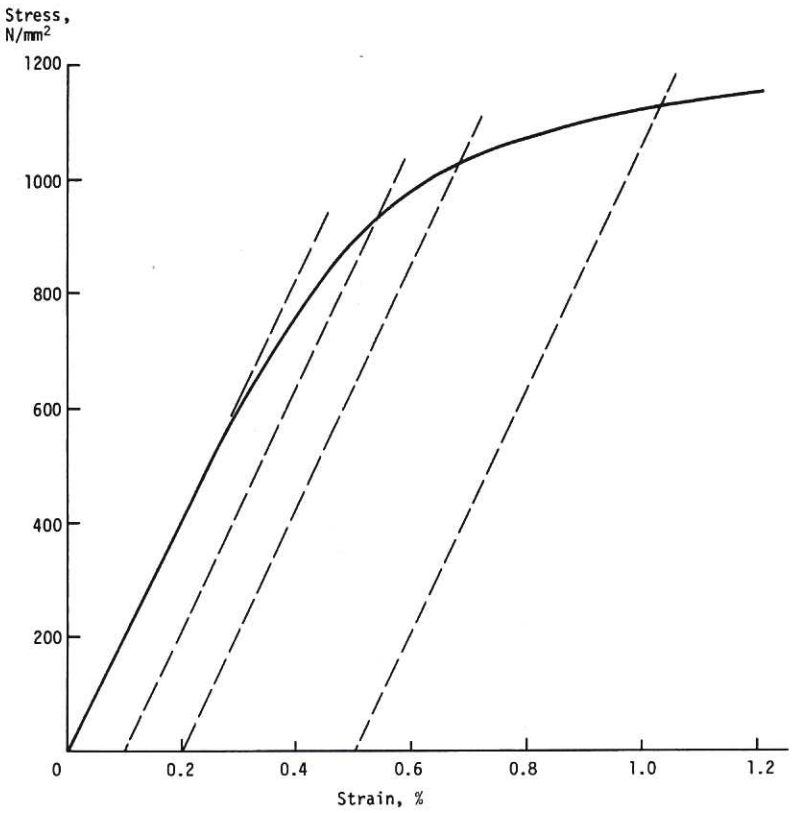

Fig.2.4 Stress-strain curve of AISI 316 LN at 4K

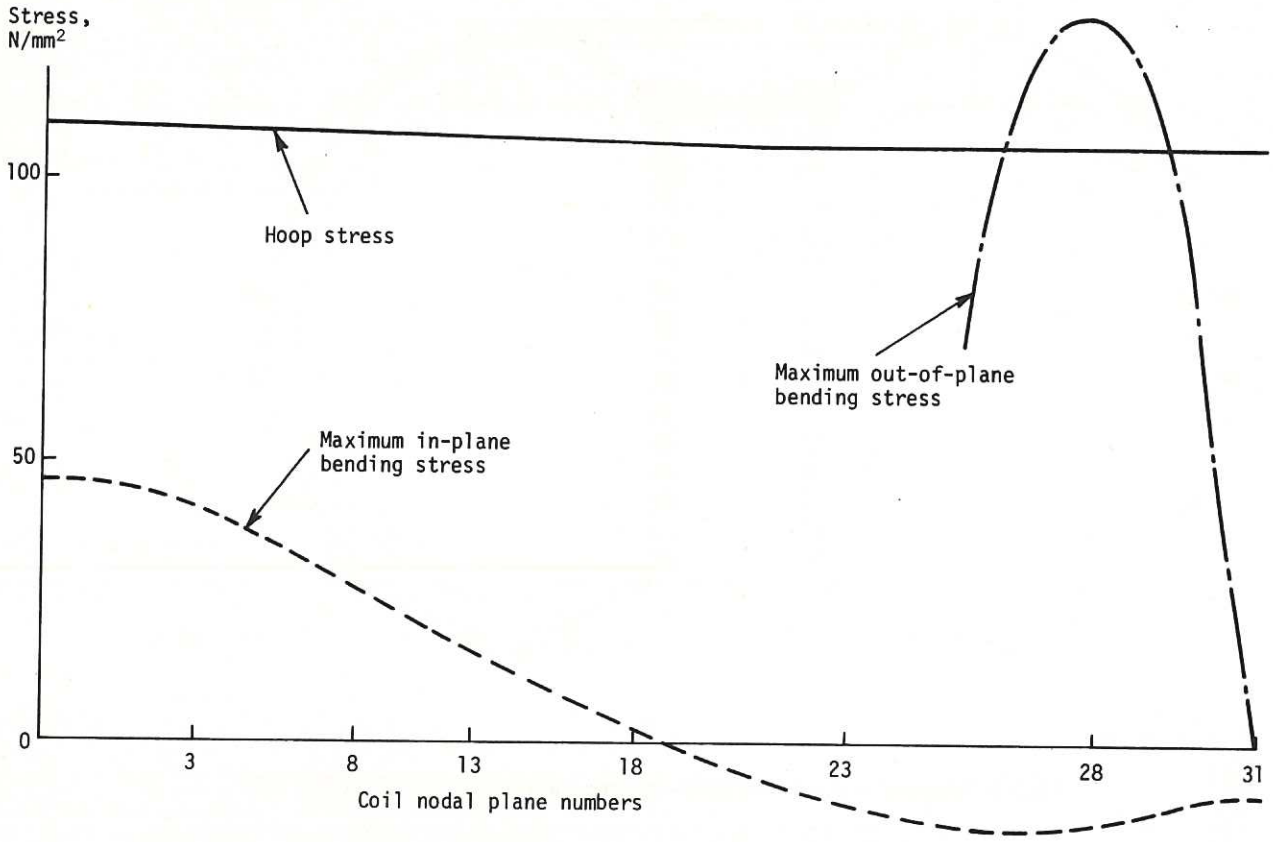

Fig. 3.1 Preliminary analysis—coil stresses for loading case L1

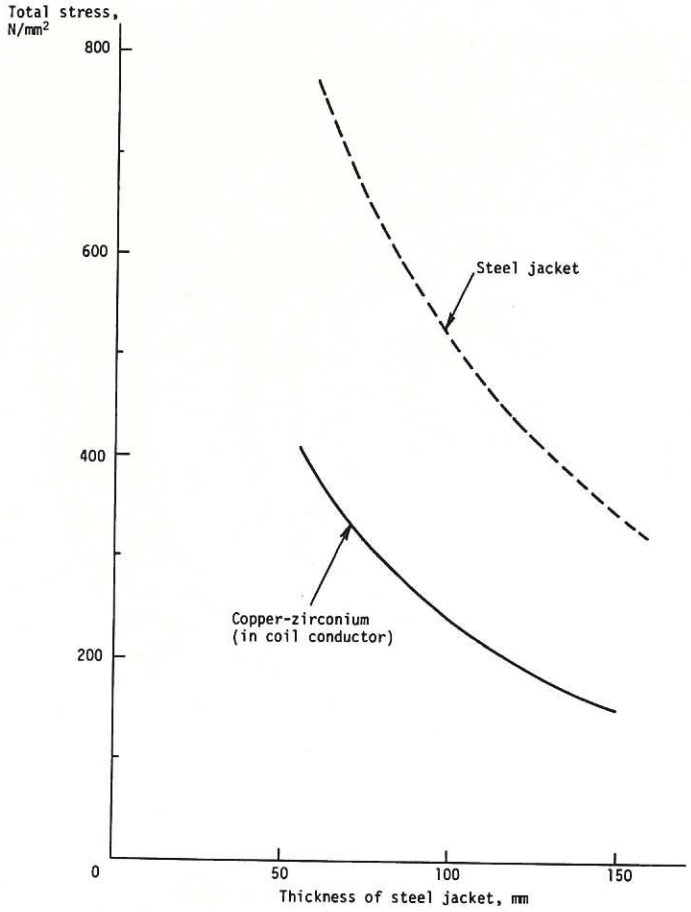

Fig. 3.2 Stresses in coil and steel jacket

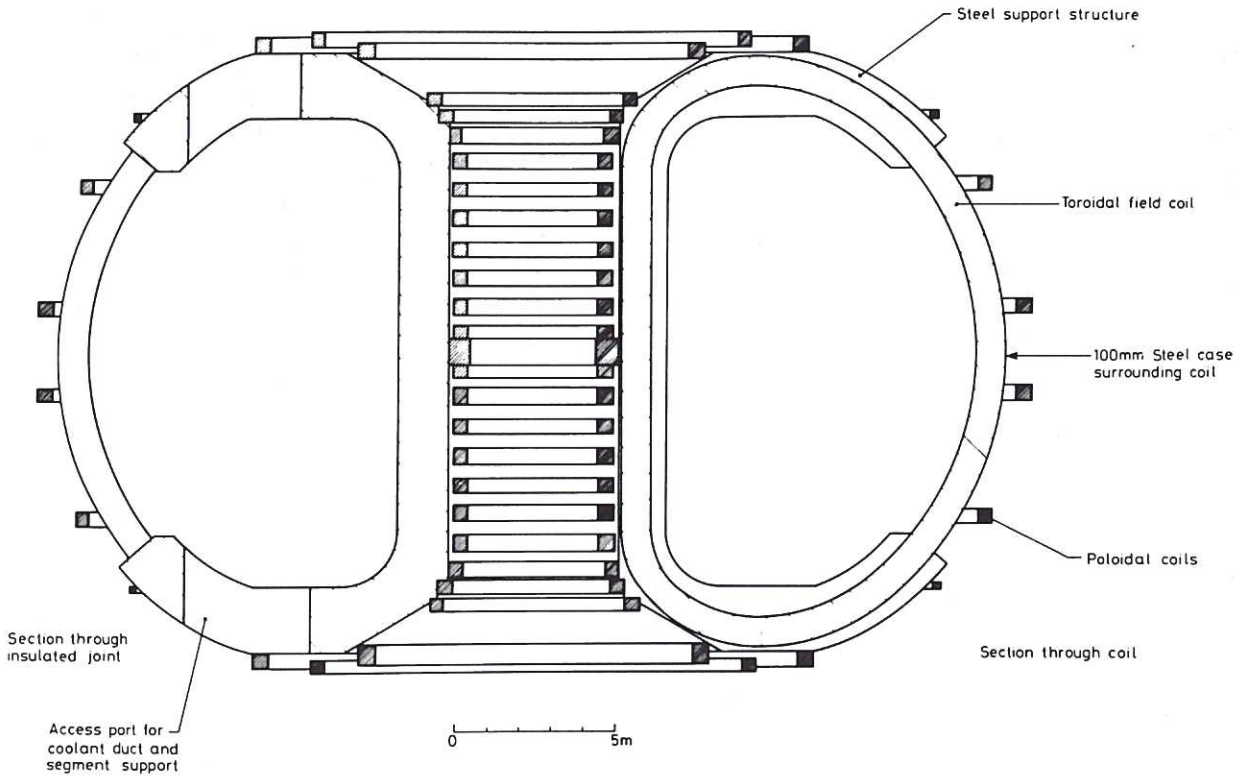

Fig.3.3 Proposed support structure—elevation along section XX′ of Fig.3.4

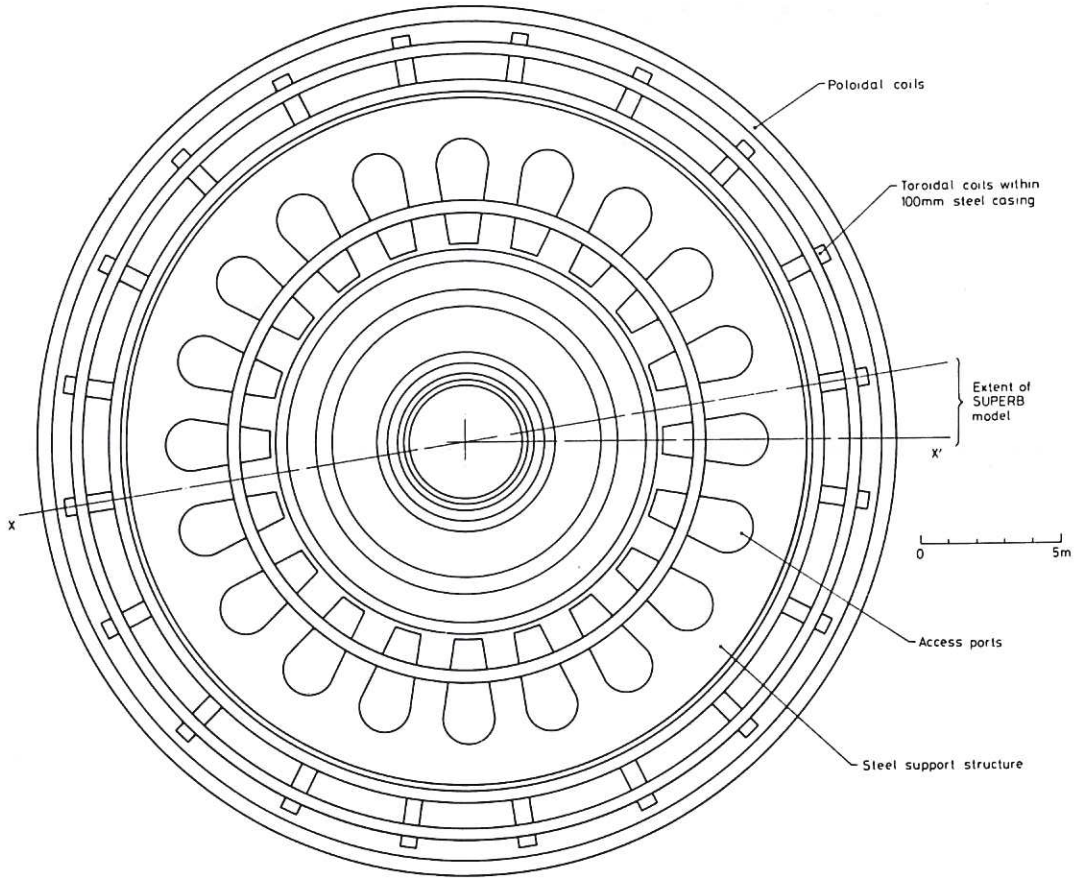

Fig.3.4 Proposed support structure—plan

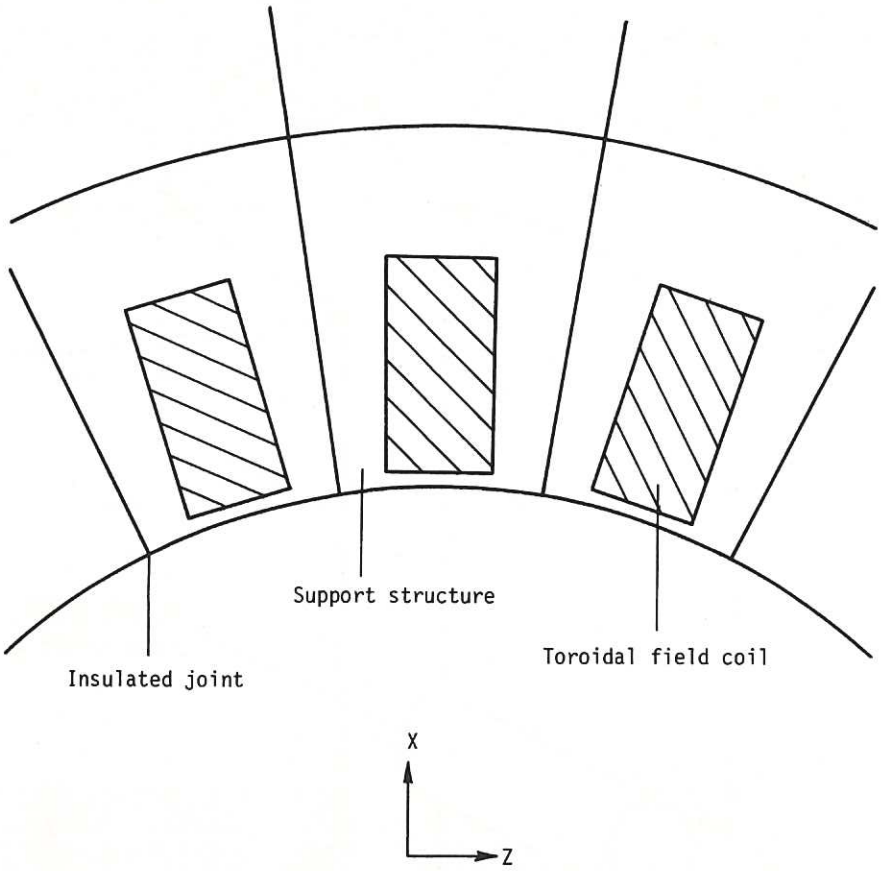

Fig. 3.5 Keystone arch structure

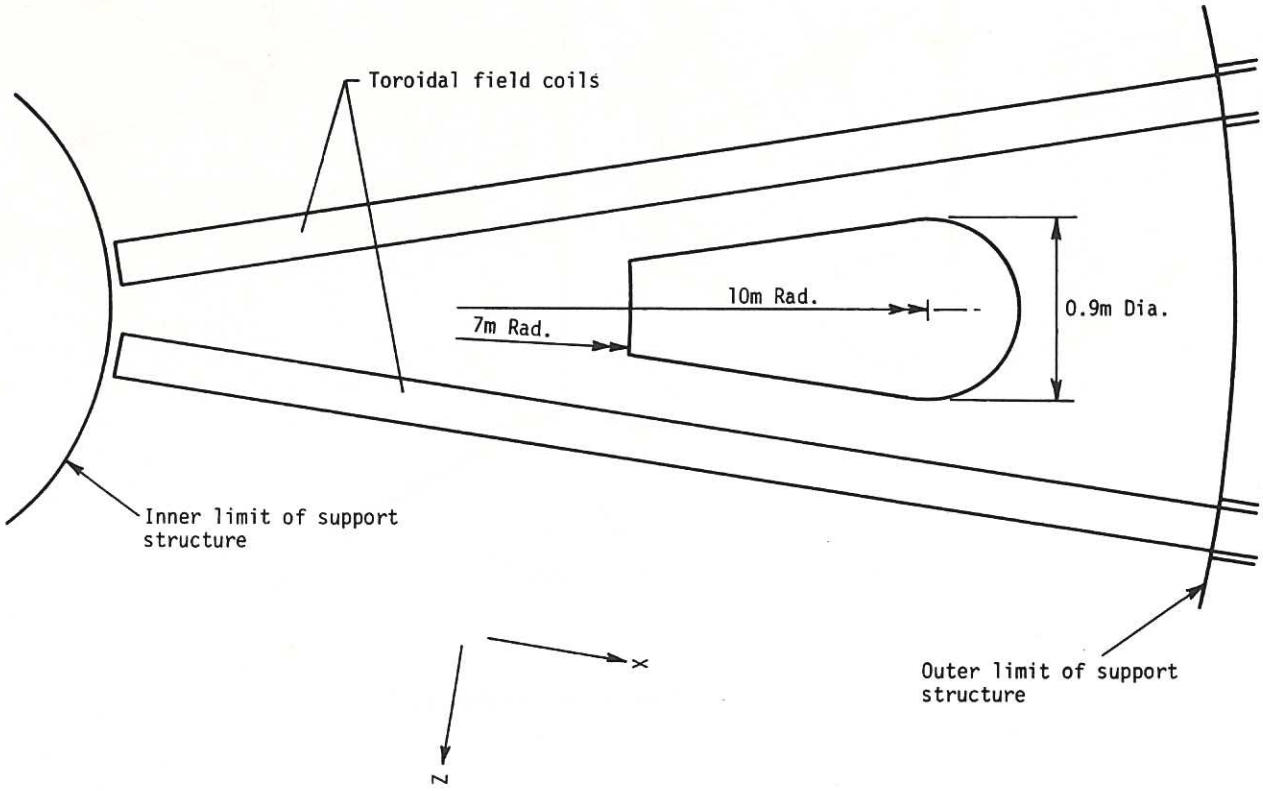

Fig. 3.6 Access region to plasma duct

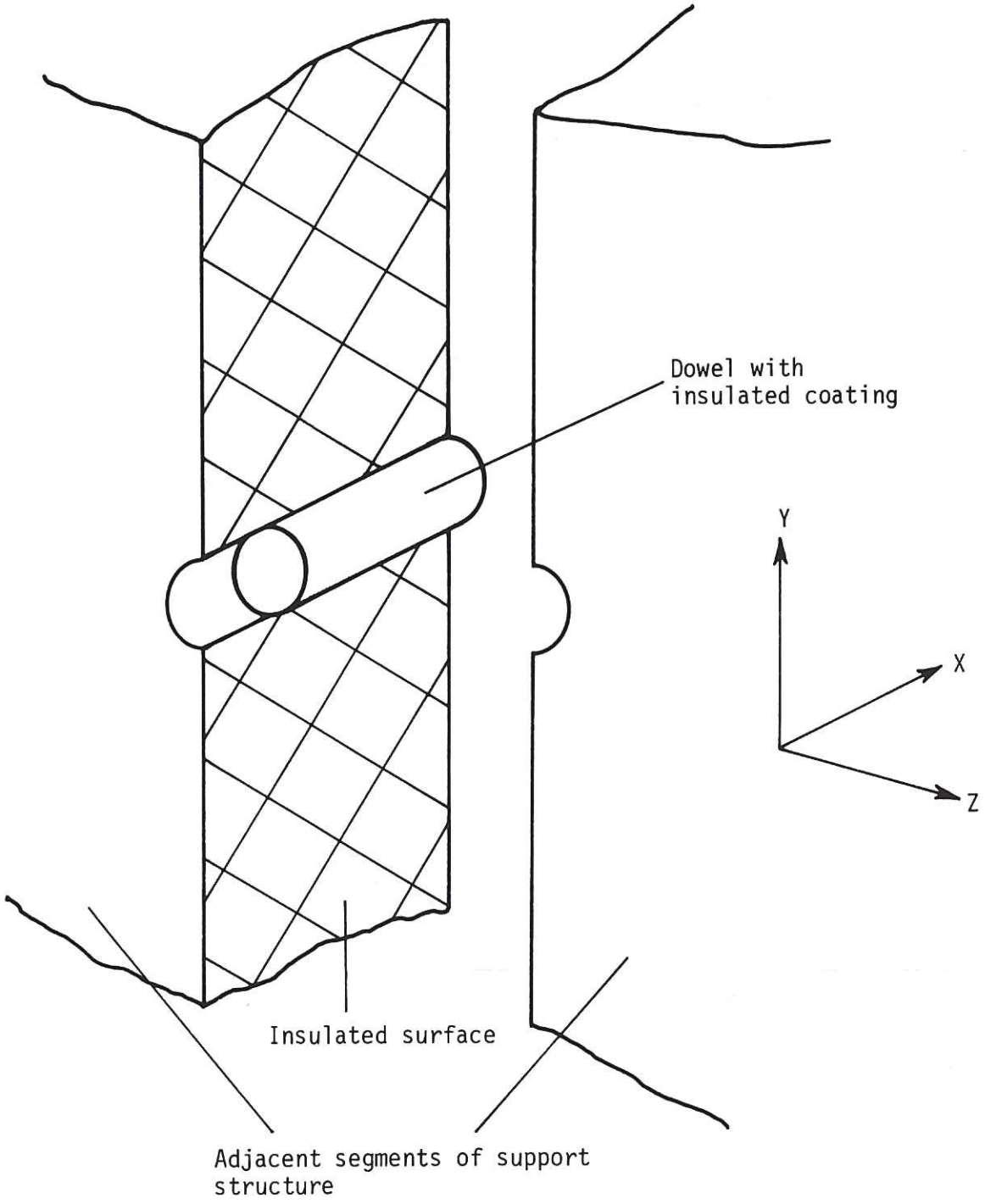

Fig. 3.7 Insulated dowel arrangement

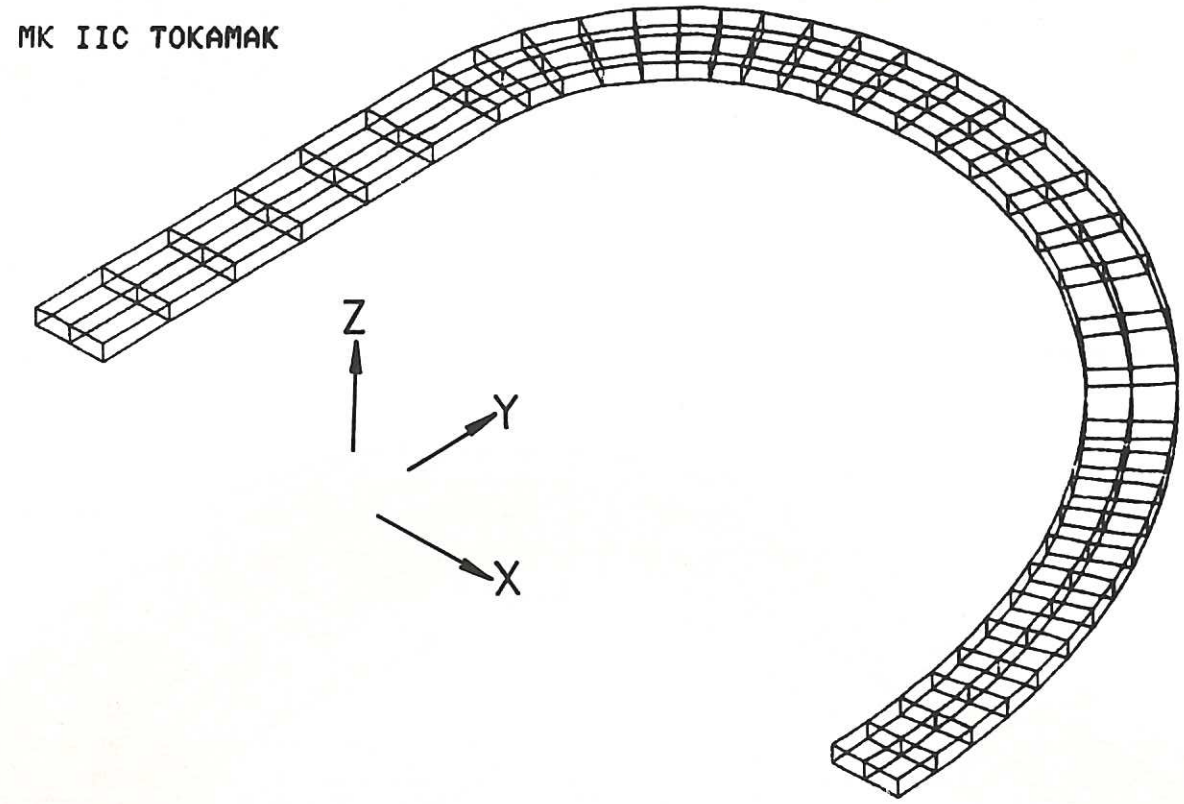

Fig.4.1 SUPERB model of coil

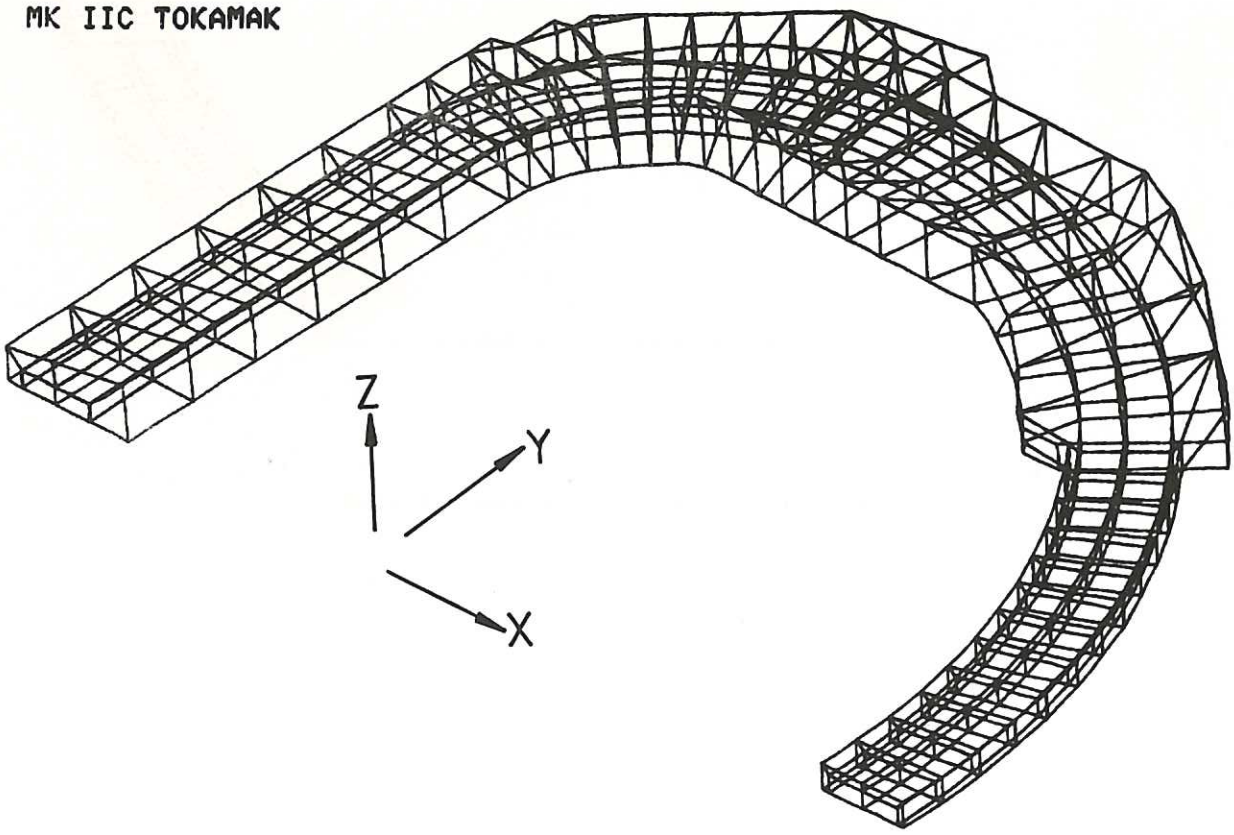

Fig.4.2 SUPERB model of coil and part of support structure

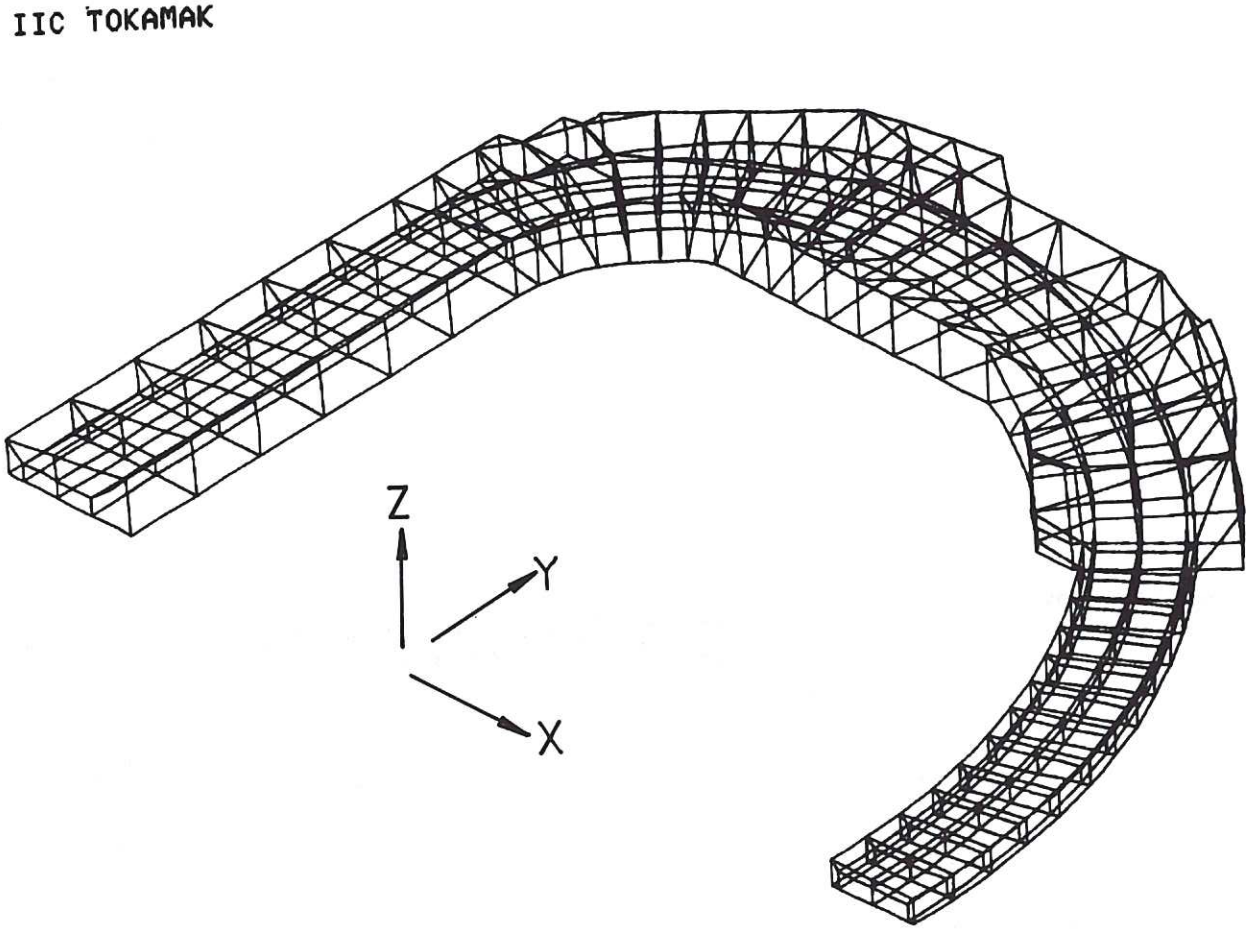

Fig. 4.3 SUPERB model of coil and support structure

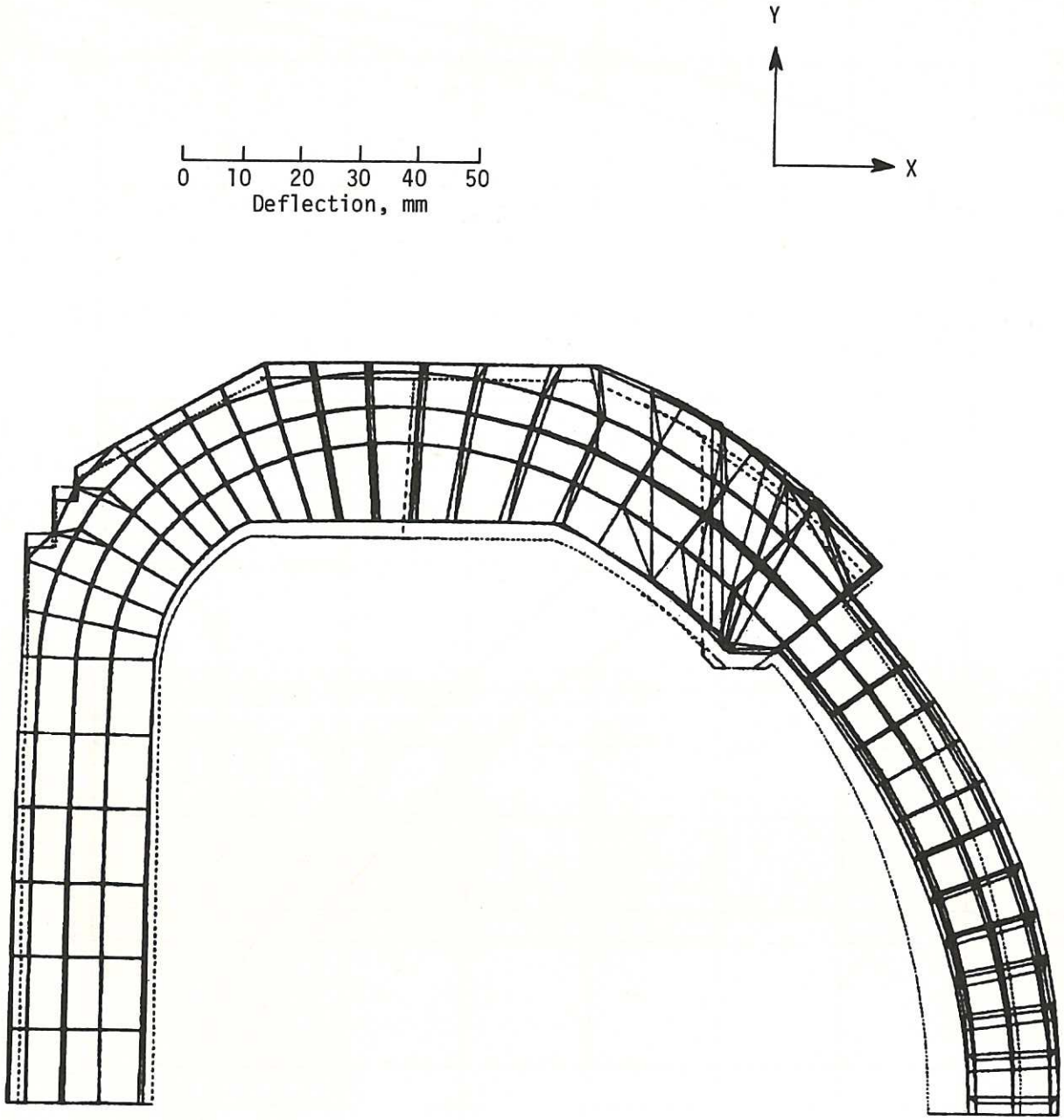

Fig.5.1 In plane deflection of structure – load case L1

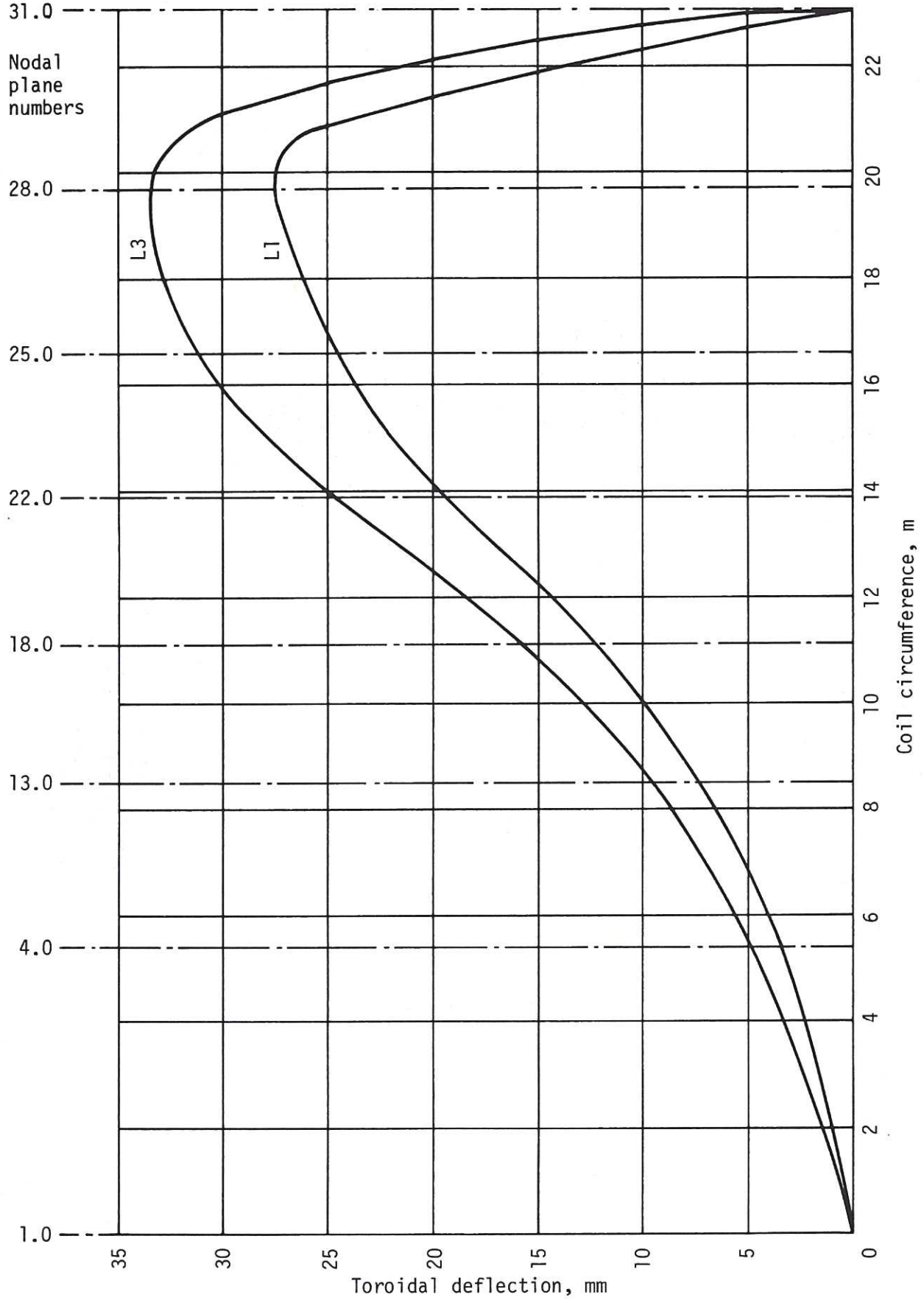

Fig.5.2 Out of plane deflection—load case L1, L3

CLM-R224

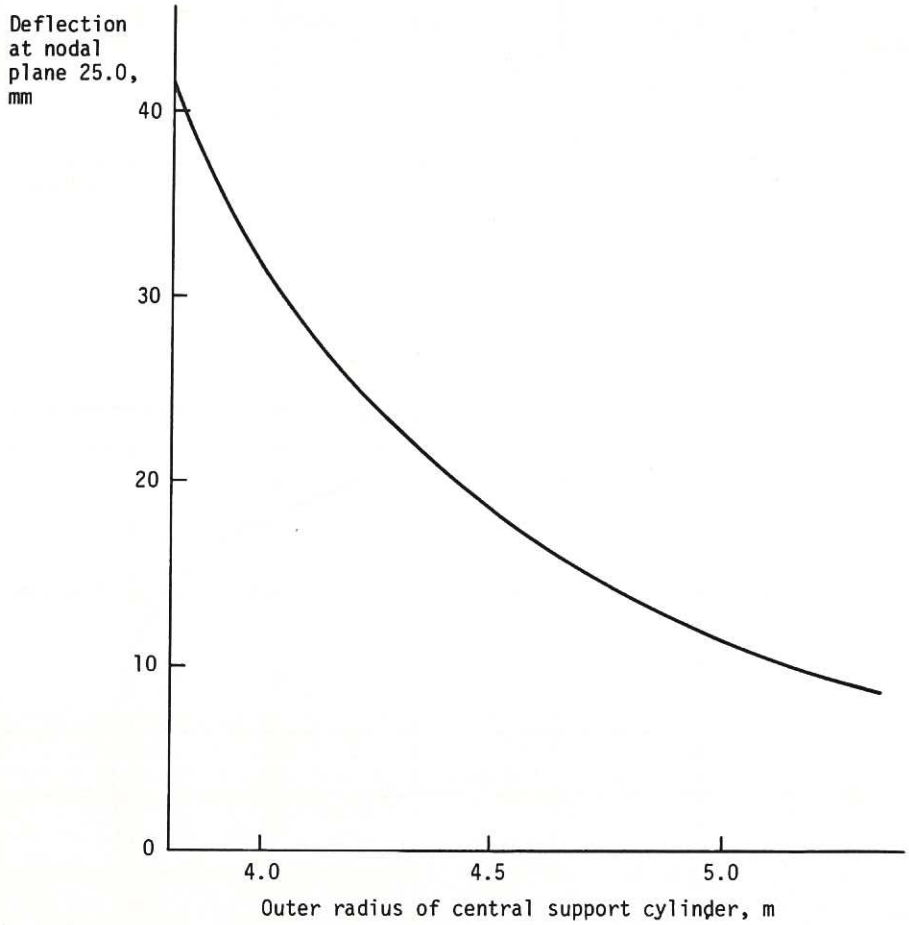

Fig. 5.3 Coil out of plane deflections—loading case L1

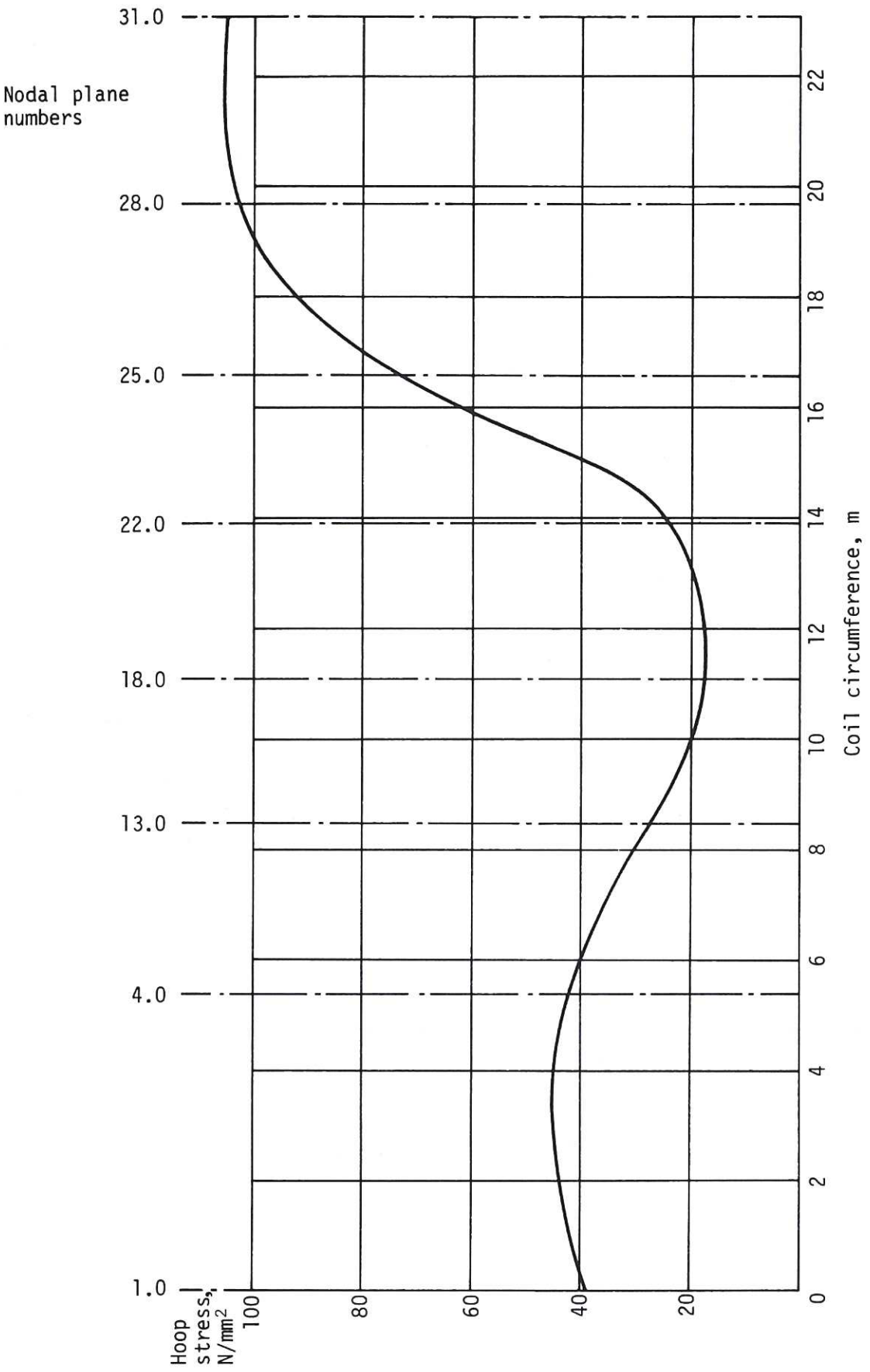

Fig.5.4 Coil hoop stress–load case L1

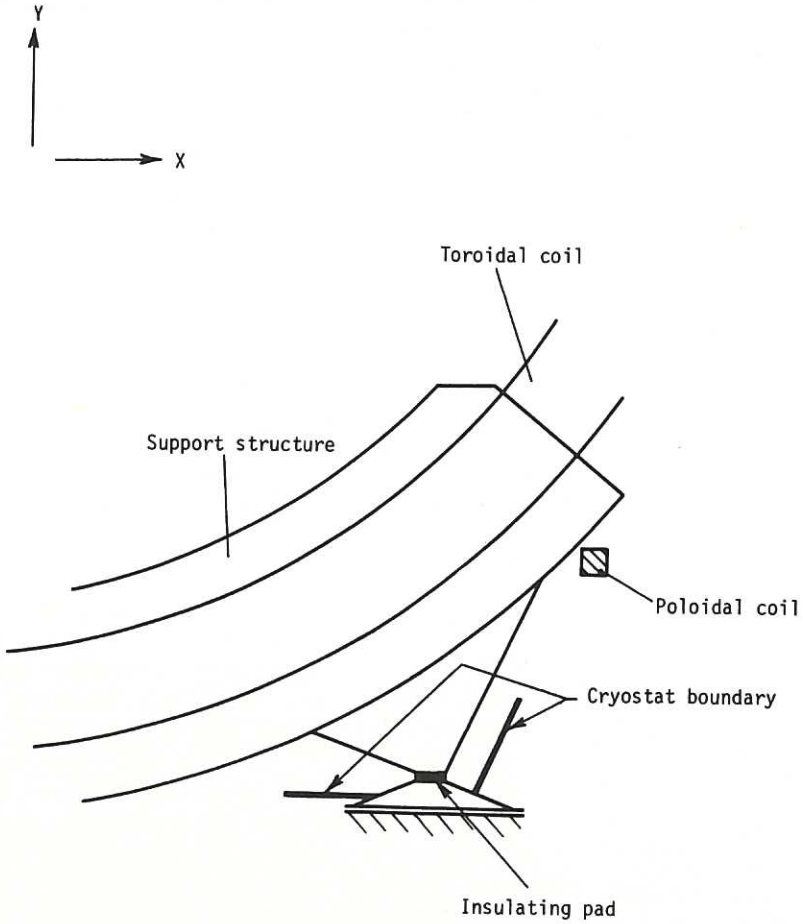

Fig.6.1 Mass support

APPENDIX A

DERIVATION OF ELASTIC CONSTANTS USED FOR COMPUTER ANALYSIS

1 MODELLING USED FOR SAGS

For this modelling, the coil was assumed to be surrounded along its entire length by a steel jacket of constant thickness. Assuming that the coil and steel are bonded together, the effective modulus, E, and second moment of area, I, of the coil/steel combination is given by:

$$E = \frac{E_c A_c + E_s A_s}{A_c + A_s}$$

$$I = I_c + \frac{E_s}{E_c} I_s \qquad \text{(A.1)}$$

where E_c, E_s are the respective moduli for copper and steel, and A_c and A_s are the corresponding cross-sectional areas. A_s can be readily calculated when the thickness of the steel jacket is known. The value of I in Equation (A.1) is that appropriate for calculating stresses in the copper-zirconium of the coil. For calculating the steel stresses the value given in Equation (A.1) must be multiplied by the ratio E_c/E_s.

A value of 0.3 was taken for the Poisson's ratio of the coil/steel combination.

Care was required in analysing the results from SAGS, since the values printed out for the stresses in the coil/steel combination are not equal to the stresses in either the copper-zirconium or the steel. In practice, the safest procedure to use is to calculate the stresses in the copper-zirconium and steel from the values, printed out by SAGS, of hoop force and bending moment along the coil.

2 MODELLING USED FOR SUPERB

Figure 2.2, in the main text of this report shows the construction of the conductor assumed for this study. Because of the highly anisotropic nature of the conductor construction, it follows that the elastic constants of the toroidal coil will have different magnitudes in different directions. To obtain reasonable values for the elastic constants, for use in the computer program SUPERB, the dimensions taken in an earlier study[2] were used. In practice some modification of these dimensions might be required for the present case.

The only load bearing constituent of the conductor is the copper-zirconium. This occupies 87.7% of the coil cross-section (see *Table 3*). Due to the presence of the cooling channels, forces in the radial and axial directions (i.e. the directions marked x_1 and x_2 in *Figure 2.2*) are effectively only carried across a fraction

f of the coil area perpendicular to the force. This has the effect of reducing the effective elastic constants of the coil in these directions. The effective modulus becomes that of copper-zirconium (E) multiplied by the fraction f. The value taken for E_c for the present study is 118 GN/m^2 (see *Table 5*).

From these considerations the Young's moduli of the coil are derived as follows.

Along coil E_1

In this case, the force is applied in a direction perpendicular to the plane of the paper in *Figure 2.2*. Of the area of the conductor 87.7% is taken up by copper-zirconium reinforcement; hence the moduli, E_1, in this direction = 0.877 x 118 GN/m^2 = 103 GN/m^2.

Radial direction E_2

In this case, the force is applied in the direction x_1 shown in *Figure 2.2*. The factor f due to the cooling channel is approximately half in this case so that the effective modulus in the radial direction = 0.5 x 118 GN/m^2 = 59 GN/m^2.

Out-of-plane direction E_3

This direction is that marked x_2 in *Figure 2.2*. The factor f due to the cooling channel is approximately two-thirds in this case, so that the effective modulus, E_3 = 0.67 x 118 GN/m^2 = 79 GN/m^2.

It was not possible during the course of the present study to arrive at a convincing derivation of the values for effective Poisson's ratio. This is due to the uncertainty caused by the anisotropic nature of the coil, and in particular the voids within the coil caused by the presence of cooling channels. These will reduce the value of Poisson's ratio to less than 0.3. The values given in *Table 6* were chosen for the present work. However, it is possible that, in future work these values may need to be modified as a result of further consideration on this topic. It is not considered however, that the precise values taken for Poisson's ratio are critical in this work. The results given in this report show that the biggest stresses generated are those along the coil (hoop stresses and bending stresses). The magnitude of these are not significantly affected by the value chosen for Poisson's ratio.

APPENDIX B

SIMPLE ANALYSIS OF STRESS DUE TO STRUCTURE MASS SUPPORT

Reference B1 considers the case of a ring uniformly loaded at W Newtons/metre circumference and supported at its base. The maximum bending stress occurs at the base and is given by:

$$\sigma = \frac{WR^2t}{I}\left[1 - \frac{k}{4}\right]$$

where R = radius of ring, t its radial depth, I = second moment of area of the ring, and

$$k = \frac{1 - 2.1\,\alpha}{1 + 4.1\,\alpha}$$

where

$$\alpha = \frac{I}{AR^2}$$

and A is the cross-sectional area of the system.

For this analysis, R has been taken as 7 m (since the perimeter of a D-shaped coil is 46 m which corresponds to an effective radius of 7.3 m). For the estimated weight of a coil and its associated structure $W = 1.5 \times 10^5$ N/m. Using values appropriate to the unsupported region, t = 0.9 m, A = 0.38 m^2 and I = 0.11 m^4 (the effective second moment of the area of the coil with 100 mm thickness of steel around it). Hence $\alpha \ll 1$ so that $k \sim 1$ hence the maximum bending stress, σ, due to the weight support is:

$$\sigma = \frac{3WR^2t}{4\,I} \qquad \text{(B.1)}$$

This should be an over-estimate since, where the coil mass is supported, the coil is stiffened not by a steel jacket of thickness 0.1 m (as is assumed in the above calculation) but by a massive steel structure of thickness 1 m. At some distance from the support point, the structure is reduced to the level assumed in the above calculation; however *Reference B1* indicates that in this region, the stresses should be less than that given by Equation (B.1).

REFERENCE

B1 ROARK, R.J., and YOUNG, W.C. Formulas for stress and strain. McGraw-Hill, 5th edition, 1975, p. 231.

APPENDIX C

SIMPLE ANALYSIS OF DEFLECTIONS

1 TORSIONAL DEFLECTION OF CENTRAL SUPPORT CYLINDER

If a cylindrical shell of inner radius, a, outer radius, b, and length, ℓ, is subjected to a toroidal torque, Γ, then the resulting deflection, Θ, (see *Figure A.C.1*) is given by[1]:

$$\Theta = \frac{2\Gamma\ell}{\pi G\,(b^4 - a^4)} \qquad (C.1)$$

where G is the shear modulus of the shell. Applying this formula to the present problem we have, a = 2.65 m, b = 4.15 m, ℓ = 8 m (i.e. modelling the upper half of the coil), G = 60 GN/m^2 (i.e. a value intermediate between the shear modulus of copper and steel, since in reality the shell consists of a keystone arch arrangement of coils, each surrounded by a steel jacket). $\Gamma = 6.4 \times 10^9$ Nm for case L1. Note that this value is 20 times the moment acting on one coil, since there are 20 coils arranged around the support cylinder, each subjected to the same moment acting in the same sense.

Application of the equation gives a value for Θ of 0.0022 radians. Thus, the outermost part of the structure at the top and bottom of the coils, which is at a radius of 12 m from the axis of the support cylinder, will experience an out-of-plane deflection of 26 mm. Reference to *Figure 5.2* shows that this is similar in magnitude to the total deflection predicted by SUPERB in this region.

2 BENDING AND SHEAR DEFLECTION OF TOP AND BOTTOM PARTS OF SUPPORT STRUCTURE

In addition to the rotation of the top and bottom parts of the structure, those parts of the structure are also subject to bending and shear deflections. For simplicity the only force assumed to be present is the net force acting on the unsupported coil region between nodal planes 25.0 and 31.0. The magnitude, F, of this force is 21 MN per coil for loading case L1. The maximum deflection occurs over the narrow region of the structure (see *Figure 3.4*) between the regions left free for access to the coolant duct. The length, ℓ, of this region is 3 m, its depth, b, in the out-of-plane direction = 1.2 m and, d, its thickness in the vertical direction is 2.0 m. Hence its stiffness, EI, against bending in the out-of-plane direction is approximately 6×10^{10} Nm^2.

From *Reference C1*, the deflection due to bending is given by:

$$y_1 = \frac{F\ell^3}{12EI}$$

$$= 0.8 \text{ mm}$$

and the deflection due to shear

$$y_2 = \frac{F\ell}{tdG}$$

$$= 0.3 \text{ mm}$$

where G is the shear modulus. A value of 8×10^{10} N/m^2, appropriate to steel, has been taken for G. Hence the net deflection of each of the top and bottom arms of the support structure is 1.1 mm.

3 BENDING OF THE UNSUPPORTED PART OF THE COIL

This part of the system can be modelled as shown in *Figure A.C.2*. The unsupported part of the coil is treated as a straight beam. The left hand end of the beam, held by an encastré fixture, represents nodal plane 25.0. From symmetry considerations, the coil behaves as though it was pin-jointed at nodal plane 31.0 and this is the representation used in the model. An imposed deflection of 25 mm (see *Section 1* of *Appendix C*) is imposed on the beam as shown in *Figure A.C.2*. The stiffness, EI, of the beam is taken as 3.9×10^9 Nm^2; this corresponds to a uniform thickness of 100 mm of steel around the coil. In the present model, a uniform loading of 3.2 MN/m is assumed to act on the beam. This corresponds to the average out-of-plane loading on the unsupported part of the coil. In reality, some variation occurs in the loading along the length of the coil; this, however, has not been represented here. The length, ℓ, of the beam has been taken as 6.4 m, approximately equal to the curved length of the neutral-axis of the unsupported part of the coil between nodal planes 25.0 and 31.0.

Although the configuration shown in *Figure A.C.2* does not represent a 'standard case', it can nevertheless be analysed by the usual methods applicable to the bending of straight beams. The main results of this analysis are that the maximum transverse displacement of the beam is 1.3 mm and occurs at a distance of 1.9 m from the encastré fixture.

In addition to this displacement due to bending of the unsupported part of the coil, there will be an additional out-of-plane displacement due to rotation of the central support cylinder (see *Section 1* of *Appendix C*). The outermost part of the neutral axis of the coil is at a radius of about 14 m from the support cylinder axis. With Θ = 0.0022 radians in Equation (C.1), this implies an out-of-plane displacement due to torsion of $\sim$ 31 mm. This increases to about 32 mm due to the bending contribution calculated above.

It is clear, therefore, that the deflection pattern of the Tokamak is dominated by the torsion in the central support cylinder due to the out-of-plane forces, and the consequent rotation of the support structure at the top and bottom of the coils.

REFERENCE

C1 ROARK, R.J., and YOUNG, W.C. Formulas for stress and strain. McGraw-Hill, 5th edition, 1975, p. 96.

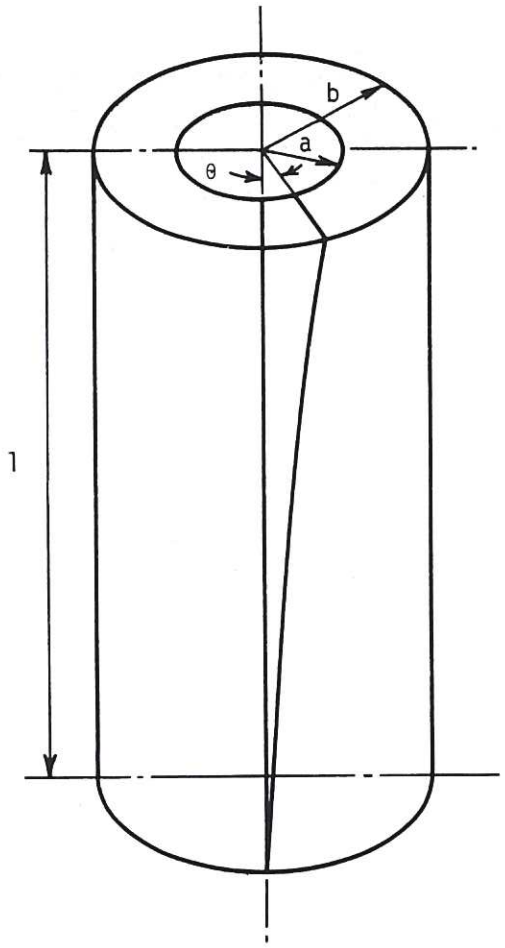

Fig.A.C.1 Torsional deflection of a shell

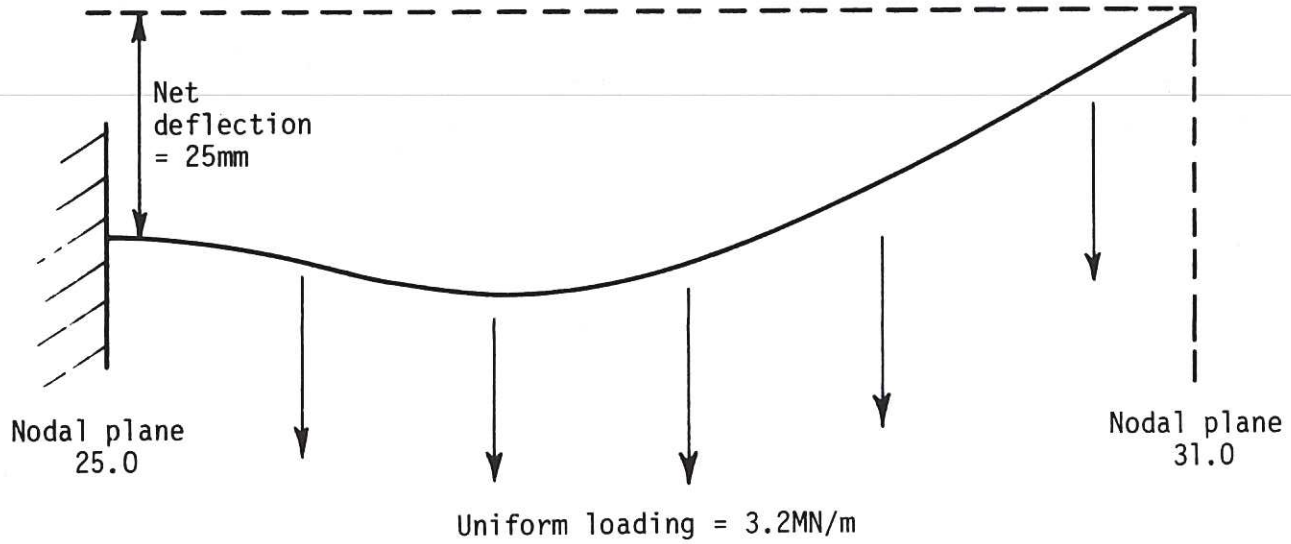

Fig.A.C.2 Deflection of unsupported part of coil

APPENDIX D

FRACTURE MECHANICS ASPECTS OF CULHAM MARK II C SUPPORT STRUCTURE

The basic principles of fracture mechanics are treated elsewhere (see *Reference D1*). The simple geometry to be considered is a pulsating unidirectional force acting on a plane crack perpendicular to the direction of the force. Under these circumstances, the rate of increase in the size of crack per cycle (da/dN) is given by:

$$\frac{da}{dN} = f\ (K_1 - K_2)$$

where K is the stress intensity factor, given by:

$$K = \lambda\sigma\sqrt{\pi a} \qquad (D.1)$$

σ is the stress at the crack and λ is a constant dependent on the crack type and geometry. For through thickness and edge cracks λ = 1.0 and 1.1 respectively and a value of 1 will be taken in this treatment. The suffixes 1 and 2 refer to the maximum and minimum stresses at the cracks during the cycle.

The form of the dependence of da/dN on the stress intensity factor range, $\Delta K = K_1 - K_2$, must be determined experimentally. Generally, crack growth does not occur (da/dN = 0) for values of ΔK below a certain threshold value, ΔK_o. When the stress intensity factor K, reaches a critical value, K_{Ic}, unstable crack growth occurs. At an intermediate region, da/dN depends on ΔK by a simple power law.

Thus, the relevant data required for even a preliminary fracture mechanics assessment are (a) the dependence of da/dN on ΔK, and (b) values of ΔK_o and K_{Ic}.

The principal structural materials considered in this study are austenitic stainless steel and copper-zirconium. The stainless steel proposed is AISI 316 LN and this appears to be the most suitable from fatigue considerations (see *Reference D2*). Fracture mechanics data on copper-zirconium do not appear to be available, but some data exist for AISI 316 LN and related steels. Published data (see *Reference D3 and D4*) on AISI 304 and 316 steel at 4 K agree with measurements made also at 4 K by IRD for 316 LN which indicates a law of the form:

$$\frac{da}{dN} = \alpha\ (\Delta K)^3 \text{ metres/cycle} \qquad (D.2)$$

Following conventional fracture mechanics practice, the units of ΔK are $MN/m^{3/2}$. In this case, experimental data indicate a value of 3.7×10^{-12} for the dimensional constant α for AISI 316 LN at cryogenic temperatures. This law appears to be at last approximately valid for values of ΔK down to 10 $MN/m^{3/2}$; hence ΔK_o is presumably less than this value. Measured values of ΔK_o for AISI 316 LN steel are not known although a value of 6 $MN/m^{3/2}$ has been proposed on theoretical grounds for 18/8 austenitic steels (see *Reference D5*). For designing a present day structure such as a turbogenerator rotor

a more conservative line would be used (i.e. a larger value for α than 3.7×10^{-12}). However this is not done here.

Combining Equations (D.1) and (D.2) and integrating:

$$\frac{1}{\sqrt{a_i}} - \frac{1}{\sqrt{a_f}} = 10^{-11} (\Delta\sigma)^3 N \qquad (D.3)$$

where a_i, a_f are the initial and final crack sizes in metres,

$\Delta\sigma$ is the stress range during cycling in MN/m^2

and N is the number of cycles to failure.

Equation (D.3) shows that the smaller the initial crack size a_i, the larger the number of cycles to failure. Ultimately, however strict the materials specification will be, the minimum assumed flaw size will be limited by the sensitivity of crack detection methods. For the present treatment, a minimum detectable crack size of 3 mm has been assumed; in practice, this would be a demanding requirement at the present time.

The final crack size, a_f, is that causing failure of the structure. *Reference D4* indicates that a value of K_{Ic} of 200 $MN/m^{3/2}$ is a reasonable requirement for AISI 316 LN. If satisfied, this would indicate that, at a stress level of 200 MN/m^2, flaws of sizes up to 0.5 m are required to cause failure. In general, therefore $a_f >> a_i$ so that Equation (D.3) may be approximated to the form:

$$N = \frac{10^{11}}{(\Delta\sigma)^3 \sqrt{ai}} \qquad (D.4)$$

This is the expression which is used in *Section 5.3* of the present report.

REFERENCES

D1 ROLFE, S.T. Use of fracture mechanics in design. International metallurgical reviews, vol. 19, 1974, p. 183.

D2 HUNTER, B.L. ETF - Magnet structural limits. Memorandum dated 27th August 1980.

D3 McHENRY, H.I., and REED, R.P. Structural alloys for superconducting magnets in fusion energy systems. Nuclear engineering and design, vol. 58, 1980, p. 219.

D4 ROBLER, R.L., and REED, R.P. Fatigue crack growth rates of structural alloys at four Kelvin. Semi-annual report on research in support of superconducting machinery. NBS publication, April 1975.

D5 CHONGHUA, Y, and MINGGAO, Y. A calculation of the threshold stress intensity range for fatigue crack propagation in metal. Fatigue of engineering materials and structures, vol. 3, no. 2, 1980, pp. 189-192.

APPENDIX E

SHEAR STRESSES IN CENTRAL SUPPORT CYLINDER DUE TO COIL TILTING MOMENTS

Figure A.E.1 shows a module of the keystone arch central support cylinder, i.e. the straight section of one coil with its abutting steel pieces. As noted in *Appendix C*, this coil is subject to a tilting moment, Y, of magnitude 3.2×10^8 Nm. This moment is resisted by the vertical shear forces F acting on the abutting faces of the keystone arch structure. The magnitude of F is given approximately by:

$$F \pi \frac{(b + a)}{20} = Y$$

where a and b are the inner and outer radii of the keystone arch structure. From *Appendix C*, a = 2.65 m and b = 4.15 m.

The mean shear stress, τ, across the abutting face is given by:

$$\tau = \frac{F}{2\ell (b - a)}$$

i.e.

$$\tau = \frac{10\ Y}{\pi\ell (b^2 - a^2)}$$

where 2ℓ is the effective height of the keystone arch structure. Because of the geometry of the coil, 2ℓ cannot be defined precisely. However, it cannot be less than 11.5 m, the length of the coil straight section. This gives, from Equation (D.1) a maximum value for τ of about 20 N/mm^2. If the shear force is taken over a fraction f of the butting area, then the shear force will be increased by a fraction f^{-1}.

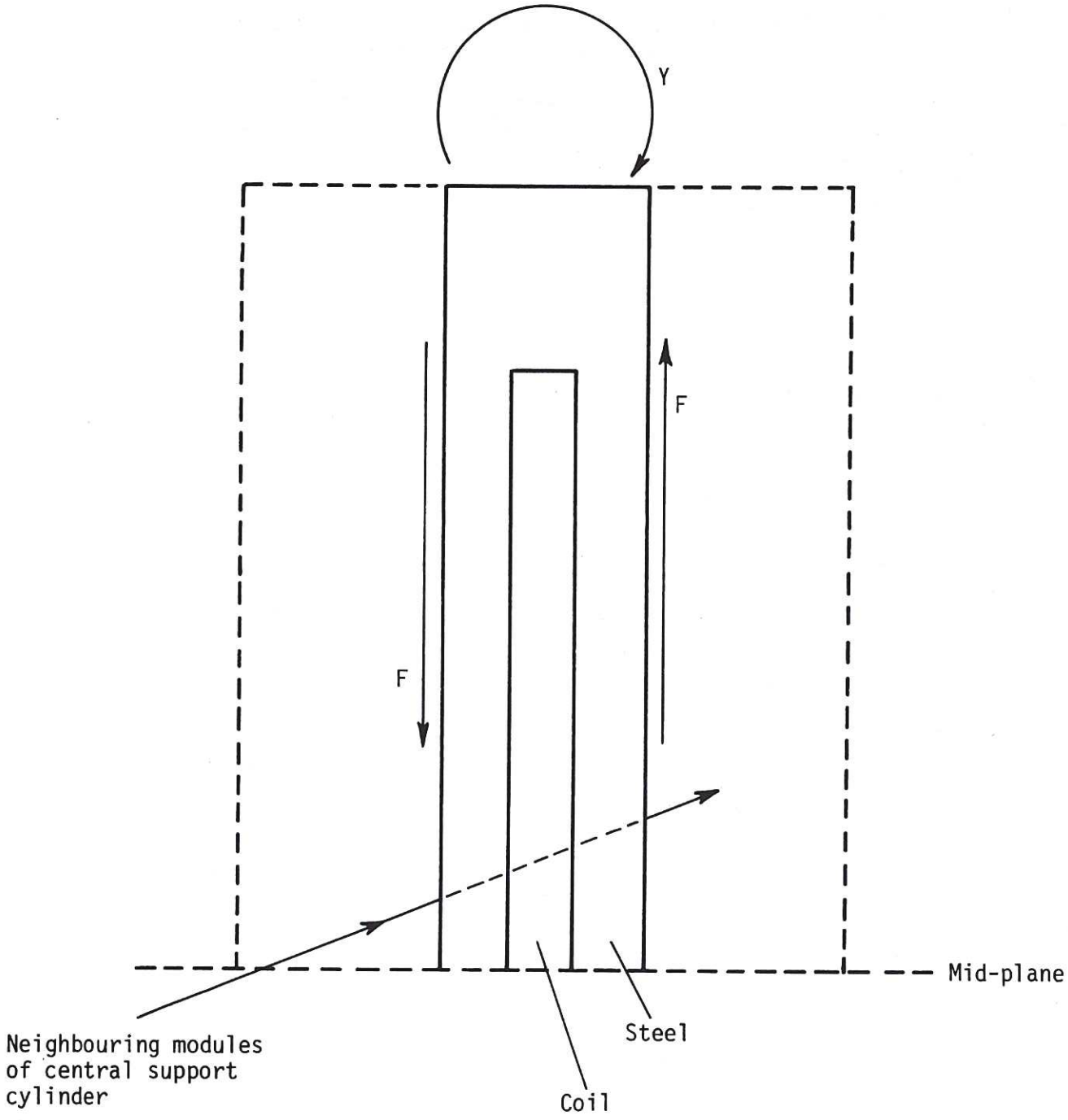

Fig.A.E.1 Shear force in central support cylinder

APPENDIX F

STRESSES ON INSULATED DOWELS

Consider a single dowel, as shown in *Figure 3.7*, with a shear force F acting on it. The overall shear stress, S, ignoring stress concentration factors, is given by:

$$S = F/dl$$

where l is the length of the dowel and d is its diameter. The force, F, also produces compression across the insulation around the dowel. This is more difficult to estimate precisely. Hence for the present work, it has been assumed that the shear load on the dowel is transmitted into the body of the structure through 25% of the surface area of the dowel. Hence the effective area is L D/4, and the resulting compressive stress, C, is:

$$C = F \frac{4}{DL} \qquad \text{(F.1)}$$

Hence $$\frac{C}{S} = \frac{4}{\pi} = 1.27$$

Although the assumption of 25% effective area is clearly an arbitrary one, the conclusion, implied in Equation (F.1), that the ratio of compressive to shear stress is a constant independent of dowel dimension and of the number of dowels is certainly valid.

HER MAJESTY'S STATIONERY OFFICE

Government Bookshops

49 High Holborn, London WC1V 6HB
(London post orders: PO Box 569, London SC1 9NH)
13a Castle Street, Edinburgh EH2 3AR
41 The Hayes, Cardiff CF1 1JW
Brazennose Street, Manchester M60 8AS
Southey House, Wine Street, Bristol BS1 2BQ
258 Broad Street, Birmingham B1 2HE
80 Chichester Street, Belfast BT1 4JY

Publications may also be ordered through any bookseller